Inorganic Chemistry

Article

pubs.acs.org/IC

# Reactions of Group 4 Amide Guanidinates with Dioxygen or Water. Studies of the Formation of Oxo Products†

Bhavna Sharma, Tabitha M. Callaway, Adam C. Lamb, Carlos A. Steren, Shu-Jian Chen, and Zi-Ling Xue*

Department of Chemistry, The University of Tennessee, Knoxville, Tennessee 37996, United States

Supporting Information

**ABSTRACT:** Reactions of the zirconium amide guanidinates $(R_2N)_2M[^iPrNC(NR_2)N^iPr]_2$ (R = Me, M = Zr, **1**; M = Hf, **2**; R = Et, M = Zr, **3**) with $O_2$ or $H_2O$ give products that are consistent with the oxo dimers $\{M(\mu\text{-}O)[^iPrNC(NR_2)N^iPr]_2\}_2$ (R = Me, M = Zr, **4**; M = Hf, **5**; R = Et, M = Zr, **6**) and polymers $\{M(\mu\text{-}O)[^iPrNC(NR_2)N^iPr]_2\}_n$ (R = Me, M = Zr, **7**; M = Hf, **8**; R = Et, M = Zr, **9**). Mass spectrometric (MS) analyses of the reactions of water in air with **1** and **2** show formation of the Zr monomer $Zr(=O)[^iPrNC(NMe_2)N^iPr]_2$ (**10**), oxo dimers **4** and **5**, and dihydroxyl complexes $M(OH)_2[^iPrNC(NMe_2)N^iPr]_2$ (M = Zr, **11**; Hf, **12**). Similar MS analyses of the reaction of diethylamide guanidinate **3** with water in air show the formation of $Zr(=O)[^iPrNC(NEt_2)N^iPr]_2$ (**13**), $Zr(OH)_2[^iPrNC(NEt_2)N^iPr]_2$ (**14**), **6**, and $\{(Et_2N)Zr[^iPrNC(NEt_2)N^iPr]_2\}^+$ (**15**). Kinetic studies of the reaction between **1** and a continuous flow of 1.0 atm of $O_2$ at 80−105 °C indicate that it follows pseudo-first-order kinetics with $\Delta H^‡ = 8.7(1.1)$ kcal/mol, $\Delta S^‡ = -54(3)$ eu, $\Delta G^‡_{358\ K} = 28(2)$ kcal/mol, and a half-life of 213(1) min at 85 °C.

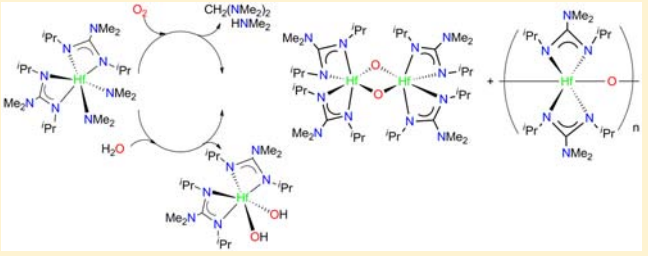

## INTRODUCTION

Many early-transition-metal complexes are sensitive to $O_2$ and $H_2O$, and they are usually handled under an inert atmosphere.[1−6] Earlier studies of the reactions between $O_2$ and early-transition-metal complexes[1] focused on O insertion into the Zr−Si bond in $Cp_2Zr(SiMe_3)Cl$[1a] and the M−C bonds in $Cp_2ZrRCl/Cp_2ZrR_2$ (R = alkyl),[1b] $(RO)_2TiMe_2$,[1c] $(Ar\text{-}O)_2TaMe_3$,[1d] and $(ArN{=})_2MoMe_2$.[1e] In addition, a bis(peroxo) complex was isolated as a product in the reaction of $O_2$ with a zirconium(IV) complex containing redox-active bis(enediamide) ligands.[2] The reaction between $O_2$ and $(ONHO)ZrCl_2(THF)$ (THF = tetrahydrofuran) with a redox-active, $H^+$-containing ligand $\{[ONOcat]^{3-}$ = bis(3,5-di-*tert*-butyl-2-phenoxy)amide$\}$ showed that the ligand served as both an electron and $H^+$ donor.[3] $O_2$ has also been used in the preparation of $d^0$ complexes. For example, $d^0$ $Mo(NMe_2)_6$ was prepared from $d^2$ $Mo(NMe_2)_4$ and $O_2$.[4] Adventitious $O_2$ was believed to play a role here in the preparation of $d^0$ complexes from $d^1$ or $d^2$ starting materials. Other reports include rapid autoxidation of $M(CH_2R)_4$ by $O_2$.[5] Our recent studies of the reactions between $d^0$ complexes and $O_2$ have revealed unusual reactivities with surprising findings.[7] Reactions of early-transition-metal complexes with $H_2O$ have also been actively studied.[8]

Reactions of $d^0$ complexes with $O_2$ or $H_2O$ have recently been used to make metal oxides as a new generation of microelectronic insulating materials through chemical vapor deposition (CVD) and atomic layer deposition (ALD) processes.[9−11] Thinner and better-insulating metal oxides make the chips smaller with better performance, and batteries in, e.g., PCs, smart phones, and tablets last longer. $HfO_2$-based chips have also been used in car propulsion systems. CVD and ALD have been used extensively to make metal oxide thin films through reactions of an oxygen source such $O_2$ or $H_2O$ with $d^0$ complexes that include homoleptic amides $M(NR_2)_n$[10a−o,11b,e,f] and imides.[10q,r] The high-oxidation-state $d^0$ complexes[1−5] show reactivities toward $O_2$ different from those of late-transition-metal $d^n$ complexes.[6] Because $O_2$ is a diradical, many of its reactions are radical in nature. For example, reactions of Group 4 $M(NMe_2)_4$ (M = Zr, Hf) with $O_2$ gave unusual aminoxides $M_3(NMe_2)_6(\mu\text{-}NMe_2)_3(\mu_3\text{-}O)(\mu_3\text{-}ONMe_2)$ and $Me_2NNMe_2$.[7a] Reactions of Group 5 $M(NR_2)_5$ (M = Nb, Ta; R = Me, Et) and $O_2$ led to insertion of $O_2$ into a M−N bond.[7b,e]

Although homoleptic Groups 4 and 5 amide complexes $M(NR_2)_n$ have been used as precursors to give metal-based materials in CVD and ALD processes,[10a−o,11b,e,f] air sensitivity of these amide precursors makes them difficult to handle. Ancillary ligands such as guanidinates have thus been used to make precursor compounds more stable.[12] As shown in Scheme 1, bidentate anionic guanidinate ligands provide at least four electrons to the metal centers.[13−15] Their zwitterionic resonance structures also contribute to the stability of the complexes. Guanidinates have been used as ancillary ligands to stabilize early-transition-metal and lanthanide complexes.[12−15] Finding new CVD/ALD precursors has led, in part, to recent interest in amide guanidinates.[13] Devi and co-workers have prepared Group 4 amide guanidinate complexes $(R_2N)_2M$-

**Received:** July 2, 2013
**Published:** September 23, 2013

  

**Scheme 1. Common Types of Bidentate N-Containing Ligands and Zwitterionic Resonance Structures of the Guanidinate Ligands**

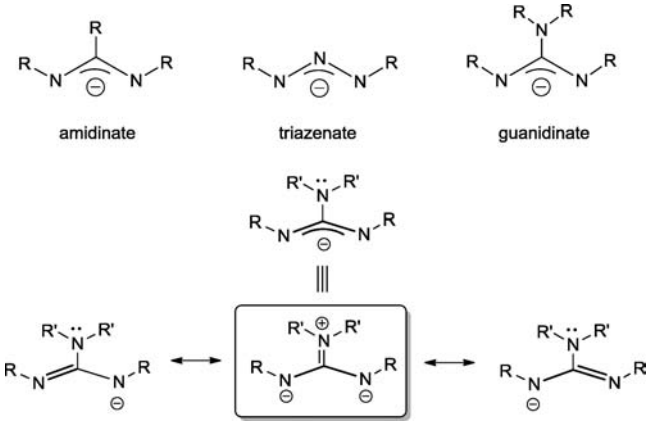


$[^{i}PrNC(NR_2)N^{i}Pr]_2$ (M = Zr, $R_2$ = $Me_2$, **1**; $Et_2$, **3**; MeEt;[12x] M = Hf, $R_2$ = $Me_2$, **2**; $Et_2$; MeEt[12l]) through insertion of $^{i}PrN{=}C{=}N^{i}Pr$ into M−$NR_2$ bonds in $M(NR_2)_4$. We have studied the reactions of $O_2$ or $H_2O$ with the guanidinate complexes **1**−**3**. The kinetics of the reaction between **1** with $O_2$ has been investigated, yielding rate constants and activation parameters $\Delta H^{‡}$, $\Delta S^{‡}$, and $\Delta G^{‡}_{358\ K}$. Our studies are reported here.

## RESULTS AND DISCUSSION

**Characterization of Group 4 Amide Guanidinate Complexes 1−3.** **1**−**3** in the current work were prepared by modified published procedures.[12l,x,16,17] Devi and co-workers have reported the crystal structures of **1** and **3**.[12x] Additional characterization of **1**−**3** is provided.[16] Detailed NMR studies of $(Et_2N)_2Zr[^{i}PrNC(NEt_2)N^{i}Pr]_2$ (**3**; Figures S1−S5 in the Supporting Information,[16] SI), including those using 2D NMR techniques, were performed to assign overlapping peaks in its $^{13}C\{^{1}H\}$ NMR spectrum, and the results are given in the SI.[16] Devi and co-workers reported variable-temperature (VT) NMR spectra of **3** at −20 to +80 °C[12x] and its hafnium analogue.[12l] We have conducted additional studies of the dynamic properties of **3** between 5(1) and 110(1) °C, yielding activation parameters $\Delta H^{‡}$ and $\Delta S^{‡}$ for the exchanges in **3**.

Analysis of the structure of **3** reveals that there are four diastereotopic centers in the compound (Figure 1) when bond rotations are restricted at 278(1) K on the $^{1}H$ NMR time scale. Similar properties have been observed by Devi and co-workers in the $^{1}H$ NMR spectra of the hafnium analogue.[12l] At 278(1) K, the $^{1}H$ NMR spectrum of **3** (Figure 1) shows four sets of doublets for the isopropyl groups $CHMe_EMe_F$ and $CHMe_GMe_H$. The $CH_AH_B$ atoms in $CN(CH_AH_BMe)_2$ on the guanidinate ligands were observed as two multiplets at 2.90−3.10 ppm. The $CH_CH_D$ atoms in the amide ligands $ZrN(CH_CH_DMe)_2$ were observed as multiplets at 3.8−3.9 ppm. A VT NMR study of **3** (Figure 1) illustrates a gradual increase in the rotations of the restricted bonds. Both $CN(CH_AH_BMe)_2$ and $ZrN(CH_CH_DMe)_2$ peaks coalesced around 333(1) K, and then each became a quartet at 383(1) K, indicating fast rotations of the N−C bonds. The isopropyl groups $CHMe_EMe_F$ and $CHMe_GMe_H$ coalesced around 338(1) and 333(1) K,

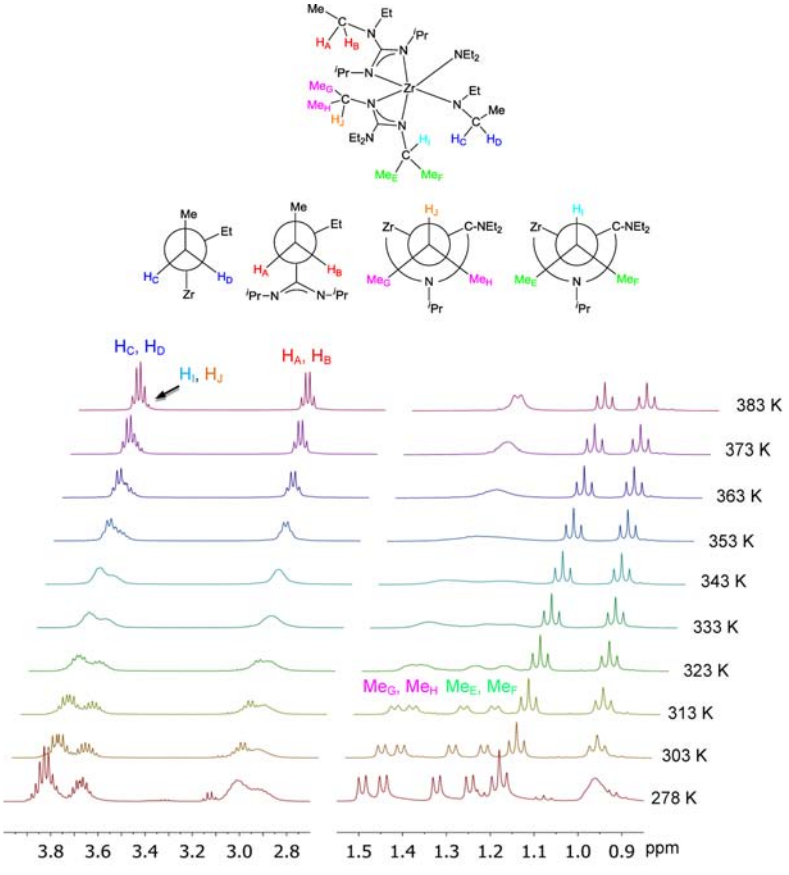


**Figure 1.** VT $^{1}H$ NMR spectra of **3** in toluene-$d_8$ showing its diastereotopic property.


dx.doi.org/10.1021/ic4016965 | Inorg. Chem. 2013, 52, 11409−11421

respectively, as a result of the fast rotation of the N−C bonds in the guanidinate ligands. Then, as the temperature increases further, the molecule undergoes Bailar exchange (Scheme 2).[18,19] The two enantiomers interconvert rapidly via a trigonal-

**Scheme 2. Bailar Twist Mechanism for Exchanges in 3**

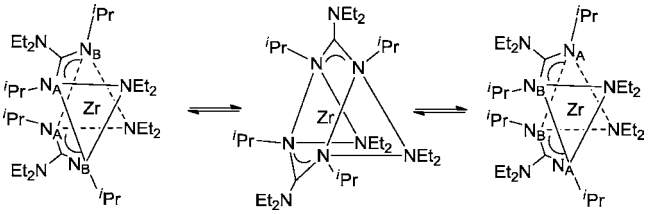

prismatic intermediate, making the two bonding sites of the guanidinate ligands equivalent. The two coalesced peaks (from CH$Me_EMe_F$ and CH$Me_GMe_H$) coalesce again at 363(1) K and eventually become a doublet at 383(1) K.

The kinetics of the exchanges in **3** has been studied. The rate constants of the interconversions in **3** at various temperatures were calculated from eq 1,[20] and they are listed in Table S1 in the SI.[16]

$$k = \pi\sqrt{2(\Delta\nu_0^2 - \Delta\nu^2)} \quad (1)$$

where $\Delta\nu$ and $\Delta\nu_0$ are the frequency differences (hertz) between exchange-broadened sites at temperature $T$ and between the two sites at the slow exchange limit, respectively.[20]

Eyring plots (Figures S6−S9 in the SI[16]) give the activation parameters of the exchanges listed in Table 1. A common

**Table 1. Activation Parameters for Interconversions in 3[16]**

| exchanges | $H_A$,$H_B$ | $Me_E$,$Me_F$ | $Me_G$,$Me_H$ | $Me_{E-F}$,$Me_{G-H}$,[a] |
|---|---|---|---|---|
| $\Delta H^{\ddagger}$, kcal/mol | 3.5(8) | 7.5(1.3) | 6.0(8) | 7.5(1.2) |
| $\Delta S^{\ddagger}$, eu | −39(2) | −27(4) | −31(3) | −26(3) |

[a] $Me_{E-F}$,$Me_{G-H}$ refers to the interconversion between $Me_E$,$Me_F$ and $Me_G$,$Me_H$ after they each have coalesced, and the interconversion eventually coalesces at 353(1) K.

feature among the four sets of activation parameters is that, in comparison to those in chemical reactions,[21] $\Delta H^{\ddagger}$ are fairly small, reflecting the fact that no bonds are broken in the exchanges. $\Delta S^{\ddagger}$ in the current exchanges are, however, much more negative than those in typical unimolecular chemical reactions, and $T\Delta S^{\ddagger}$ are, in fact, much larger contributors to the activation free energy $\Delta G^{\ddagger}$. For example, for the exchange of $H_A$,$H_B$, $\Delta H^{\ddagger}$ = 3.5(8) kcal/mol and $\Delta S^{\ddagger}$ = −39(2) eu. At coalescence [338(1) K], $\Delta G^{\ddagger} = \Delta H^{\ddagger} - T\Delta S^{\ddagger}$ = 16.7(1.5) kcal/mol. The large, negative activation entropies in the current exchanges are consistent with the difficulties in rotating the bonds and groups in the crowded molecules of **3**.

The assignments of $H_A$,$H_B$, $H_C$,$H_D$, $Me_E$,$Me_F$, and $Me_G$,$Me_H$ are supported by NOESY (nuclear Overhauser effect spectroscopy) and EXSY (exchange spectroscopy) studies.[16] $^1$H−$^1$H COSY (correlation spectroscopy) was also obtained to understand the structural features of **3**.[16] A discussion of these results is given in the SI,[16] along with the $^{13}$C{$^1$H} NMR spectrum of **3**, its peak assignments, and confirmation of the assignments by HSQC (heteronuclear single quantum coherence) and HMBC (heteronuclear multiple-bond correlation spectroscopy) experiments.

**Reaction of $(Me_2N)_2Zr[^iPrNC(NMe_2)N^iPr]_2$ (1) with $O_2$.** The zirconium amide guanidinate complex **1** has been found to react with $O_2$ slowly even at 70 °C. $^1$H NMR monitoring showed that it took ca. 44 h to complete the reaction of **1** with 1 atm of $O_2$ in benzene-$d_6$ at 70 °C. In the process, the peak of **1** gradually decreased. In solution, organic products $HNMe_2$ and $CH_2(NMe_2)_2$ (**16**) were observed in the $^1$H and $^{13}$C{$^1$H} NMR spectra (Figure S10 in the SI[16]). The *soluble*, zirconium-containing product was identified as $\{Zr(\mu\text{-}O)[^iPrNC(NMe_2)N^iPr]_2\}_2$ (**4**), the dimer of the oxo compound $Zr(=O)[^iPrNC(NMe_2)N^iPr]_2$ (**10**). An insoluble product precipitated from the solution and was identified as $\{Zr(\mu\text{-}O)[^iPrNC(NMe_2)N^iPr]_2\}_n$ (**7**), the polymer of the oxo product **10** (Scheme 3). As the reaction progressed, more precipitate formed, although the peaks of the dimer **4** stayed at about the same intensity.

The $^1$H NMR spectrum of the dimer **4** (Figure S10 in the SI,[16] top) shows two doublets at 0.885 and 1.12 ppm for the methyl groups in the isopropyl moieties on the guanidinate $[^iPrNC(NMe_2)N^iPr]^-$ ligand. The singlet at 2.64 ppm is assigned to the CN$Me_2$ methyl groups in the guanidinate ligand. The C$H$Me$_2$ atom in the isopropyl moieties appear as a multiplet at 3.30 ppm. These observations, suggesting that the two guanidinate ligands are chemically equivalent and that there are two environments for the isopropyl groups on the guanidinate ligands, are consistent with the structure of the dimer **4** in Scheme 3. One N atom of each guanidinate $[^iPrNC(NMe_2)N^iPr]^-$ ligand is trans to the bridging oxo ligands, and the other N atom is trans to the N atom of the other guanidinate ligand. The $^{13}$C{$^1$H} NMR spectrum of **4**

**Scheme 3. Reactions of $O_2$ with 1−3 and $H_2O$ with 1 and 2**

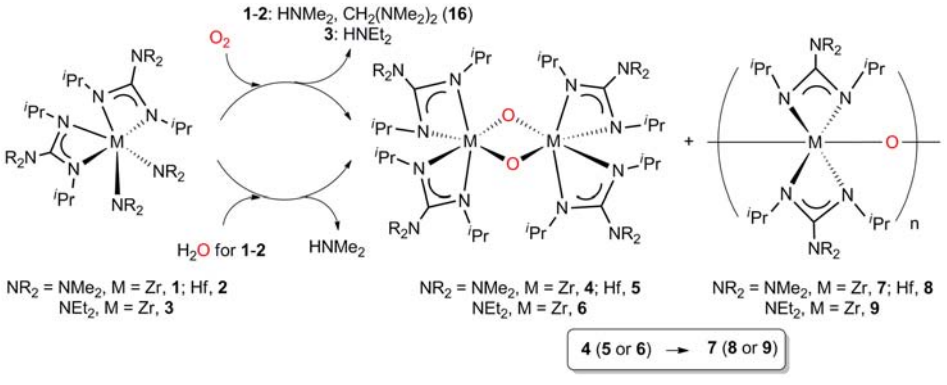



dx.doi.org/10.1021/ic4016965 | Inorg. Chem. 2013, 52, 11409−11421

(Figure S10 in the SI,[16] bottom) is consistent with the structure. Two peaks at 25.66 and 25.70 ppm are assigned to methyl groups in the isopropyl $CHMe_2$ moieties, and their CH groups are observed at 46.16 and 47.70 ppm. The peaks at 39.69 and 168.97 ppm are assigned to the methyl groups in the $CNMe_2$ moiety on the guanidinate $[^iPrNC(NMe_2)N^iPr]^-$ ligand and its quaternary C atom, respectively. Attempts to crystallize the soluble dimer **4** failed because it gradually turned into the insoluble polymer **7** and precipitated from the solution. This observation is perhaps not surprising because the dimer may polymerize into **7**, as shown in Scheme 3. The polymer **7**, however, does not dissolve in pentane, hexanes, benzene, $Et_2O$, THF, or toluene.

It should be noted that the NMR spectrum of the dimer **4** also fits the structure of the monomer, trimer, or tetramer of **10** or the polymer **7**. However, the following observations support the assignment of the species as the dimer **4**: (a) As discussed below, the dimer **4** has also been observed in the reaction of **1** with $H_2O$ and identified by its mass spectrometry (MS) spectrum. No other oligomers were observed. (b) Although both the monomer **10** and dimer **4** have been observed by MS in the reaction of **1** with $H_2O$, the pentacoordinated monomer **10** is coordinatively unsaturated and perhaps less stable than the hexacoordinated dimer **4**. (c) We cannot rule out that the soluble species is the trimer of **10** (Scheme 4), which is also hexacoordinated. However, it is unlikely to be the tetramer of **10** (Scheme 4) because it is heptacoordinated and more crowded than the dimer or trimer.

**Scheme 4. Hexacoordinated Trimer and Heptacoordinated Tetramer of 10**

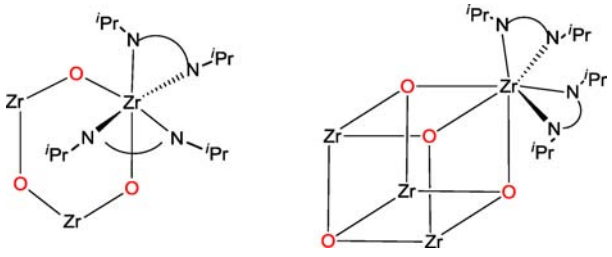


Identification of the polymer **7** was based on the solid-state $^{13}C$ NMR spectrum and elemental analysis of samples from the reaction of **1** with $H_2O$, as discussed below. Identification of $HNMe_2$ and **16** as products in the reaction was based on a comparison of the $^1H$ and $^{13}C\{^1H\}$ NMR spectra of the reaction mixture (Figure S10 in the SI[16]) with those of pure $HNMe_2$ and **16**. When the volatiles of the reaction mixture were removed in vacuo, condensed, and analyzed by gas chromatography (GC)−MS, both $HNMe_2$ and **16** were identified.

The formation of $HNMe_2$ and **16** suggests a radical nature of the reaction between **1** and $O_2$ (Scheme 3).[22] We earlier reported that the reactions of $M(NMe_2)_4$ (M = Zr, Hf) with $O_2$ gave aminoxides $M_3(NMe_2)_6(\mu\text{-}NMe_2)_3(\mu_3\text{-}O)(\mu_3\text{-}ONMe_2)$ and $Me_2NNMe_2$ (Scheme 5).[7a] Density functional theory calculations suggest a mechanism involving $^\bullet NMe_2$ radicals from homoleptic cleavage of newly formed $ZrO-NMe_2$ bonds.[7a] Several other studies have demonstrated that, once $^\bullet NMe_2$ radicals are formed, their reactions lead to the formation of $HNMe_2$ and **16** involving intermediates such as $CH_3^\bullet$, $CH_2{=}NH$, $H^\bullet$, $CH_3N{=}CH_2$, and $(CH_3)_2N-CH_2^\bullet$.[22b] Such a

**Scheme 5. Reactions of $M(NMe_2)_4$ (M = Zr and Hf) with $O_2$[7a]**

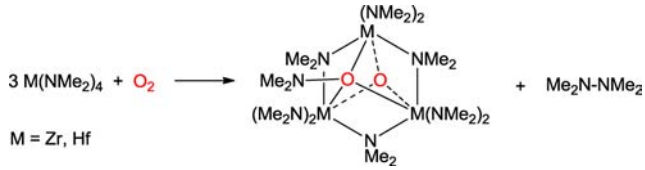


pathway may operate in the current reaction of **1** with $O_2$ in Scheme 3, giving $HNMe_2$ and **16**.

**Reaction of 1 with $H_2O$.** The reaction was initially monitored by $^1H$ NMR spectroscopy. The addition of 2 equiv of $H_2O$ in THF to **1** (15 mg) in benzene-$d_6$ was found to give soluble products $HNMe_2$ and dimer **4** (Figure S11 in the SI[16]). The reaction was much faster than that of **1** with $O_2$ and was completed in a few minutes. After the reaction, the product mixture turned slightly cloudy, presumably as a result of recipitation of the polymer **7**, but the amount of the solid was too small to be isolated. These observations point to the reaction in Scheme 3. When the reaction of **1** with water was conducted on a larger scale in THF, a $H_2O$/THF mixture (2 equiv of $H_2O$) was added to a solution of **1** in THF at 0 °C. Afterward, the solution was gradually warmed to room temperature with formation of the polymer solid **7**. The white solid was isolated by filtration and characterized by elemental analysis and IR and solid-state $^{13}C$ NMR spectroscopies. Volatiles in a small amount of filtrate were removed in vacuo. $^1H$ and $^{13}C\{^1H\}$ NMR analyses of the residue showed that it was mainly the dimer **4**. Attempts to grow crystals from the filtrate yielded additional insoluble solid of the polymer **7**.

The solid-state $^{13}C$ NMR spectrum of **7** (Figure S12 in the SI[16]) shows peaks at 23.67 ppm for $CHMe_2$, 39.93 ppm for $C-NMe_2$, 45.65 ppm for $CHMe_2$, and 159.17 ppm for $CNMe_2$. These resonances are consistent with the polymeric structure of **7**. It is noted that one peak at 23.67 ppm is observed for the methyl groups on the $CHMe_2$ moieties on the guanidinate $[^iPrNC(NMe_2)N^iPr]^-$ ligand. Although we cannot rule out the possibility that two $CHMe_2$ peaks overlap here, the observation of a single peak is consistent with the structure of the polymer **7** in Scheme 3, in which all four $CHMe_2$ groups on a Zr center are chemically equivalent. In comparison, there are two inequivalent $CHMe_2$ groups in the dimer **4** (Scheme 3), as revealed by its NMR spectrum (Figure S10 in the SI). Similarly, the trimer of **10** would also have two inequivalent $CHMe_2$ groups (Scheme 4). In addition, the trimer is expected to have some solubility in common organic solvents. As analyzed earlier, the heptacoordinated tetramer of **10** (Scheme 4) is more crowded, and it is unlikely to be a product. These analyses, including elemental analysis and the insolubility of **7**, support its assignment as a polymer. The IR spectrum of **7** in a KBr pellet (Figure S13 in the SI[16]) revealed a peak at 1625 $cm^{-1}$ in the typical range of the C=N stretching frequencies between 1690 and 1640 $cm^{-1}$.

Why is the reaction of **1** with $H_2O$ here fast? Schwartz and co-workers have found that the reactions of $Zr(O^tBu)_4$ with surface OH groups are faster than those of its alkyl analogue $Zr(CH_2{}^tBu)_4$.[8a] Lone-pair electrons on $O^tBu$ assist $H^+$ migration from the OH groups to the alkoxide ligand, removing the latter. The amide ligands $NMe_2$ in **1** also contain lone-pair electrons, and they may help with $H^+$ migration and removal of the amide ligands (Scheme 6).


dx.doi.org/10.1021/ic4016965 | Inorg. Chem. 2013, 52, 11409−11421

**Scheme 6. $H^+$ Transfer Assisted by Lone-Pair Electrons on Amide Ligands**

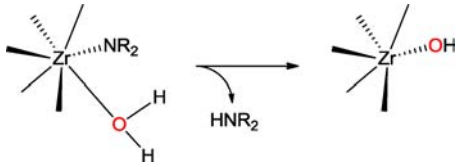


**MS Studies of the Reaction between 1 and $H_2O$ in Air.** Operations of many mass spectrometers require the exposure of samples to air, albeit briefly (in a few seconds). Thus, they are usually not appropriate for MS analyses of air-sensitive compounds, unless the mass spectrometers are operated with an inert gas apparatus.

Because the reaction of **1** with $H_2O$ had already been studied (Scheme 3), it was felt that perhaps the exposure of **1** to air during the MS operations could be utilized to observe reaction products by MS. Even though 21% of air is $O_2$, it is unlikely that there would be a significant degree of the reaction between **1** and $O_2$ during a few seconds of exposure of **1** to air at 23 °C. As discussed earlier, the reaction of **1** with $O_2$ is probably too slow at this temperature to be observed.

Zirconium is an element with five stable isotopes [$^{90}$Zr, 51.45(2)%; $^{91}$Zr, 11.22(2)%; $^{92}$Zr, 17.15(1)%; $^{94}$Zr, 17.38(2)%; $^{96}$Zr, 2.80(1)%], and MS spectra of zirconium compounds containing, e.g., one and two Zr atoms thus each show unique isotopic patterns. The analysis will help to identify whether the compound contains a Zr atom or not and how many Zr atoms are present in the compound.

Molecules of **1** reacted with $H_2O$ in air, and transient products [M + $H^+$] (species + $H^+$) were then analyzed by MS. In addition to the monomer **10** and dimer **4**, the dihydroxyl complex $Zr(OH)_2[^iPrNC(NMe_2)N^iPr]_2$ (**11**) was present (Scheme 7). The calculated mass for [**10** + $H^+$] was $m/z$ 447.23889, and the cation was observed at $m/z$ 447.24075. The isotopic patterns for both calculated and observed [monomer + $H^+$] cations are shown in Figure 2. Similarly, the calculated and observed cations of [**11** + $H^+$] for the dihydroxyl product **11** were $m/z$ 465.24945 and 465.24985, respectively, and are given in Figure 3. One pathway to the formation of the monooxo complex **10** is likely dehydration of the dihydroxyl **11**. The dimer **4**, containing two Zr atoms, has a different isotopic pattern, as shown Figure 4. The calculated [**4** + $H^+$] was $m/z$ 893.46995, and it was observed at $m/z$ 893.48166.

**Kinetic Studies of the Reaction between 1 and $O_2$.** The reaction of **1** with $O_2$ is slow even at elevated temperatures. This offers an opportunity to study the kinetics of the reaction. The reaction between **1** and $O_2$ in Scheme 3 likely follows second-order kinetics (eq 2)

$$-\mathrm{d}[\mathbf{1}]/\mathrm{d}t = kp_{O_2}[\mathbf{1}] \quad (2)$$

where $k$ = rate constant, $p_{O_2}$ = partial pressure of $O_2$, and [**1**] = concentration of **1**. Under a constant $O_2$ pressure, $p_{O_2}$ = 1 atm, the rate law in eq 3 may be simplified to

$$-\mathrm{d}[\mathbf{1}]/\mathrm{d}t = k'[\mathbf{1}], \quad \text{where } k' = kp_{O_2} \quad (3)$$

The reaction thus follows pseudo-first-order kinetics with rate constant $k'$.

The kinetics of the reaction between **1** and 1 atm of $O_2$ in toluene-$d_8$ was conducted using a home-designed apparatus (Figure S14 in the SI[16]). Experiments for seven temperatures, 353−383 K, were conducted. Plots of ln $[\mathbf{1}]/[\mathbf{1}]_0$ ($[\mathbf{1}]_0$ = initial concentration of **1**; Figure S15 in the SI[16]) yield rate constants $k'$ in Table 2. The Eyring plot $\ln(k'/T)$ versus $1000/T$ (Figure S15 in the SI[16]) gives the activation parameters $\Delta H^‡$ = 8.7(1.3) kcal/mol, $\Delta S^‡$ = −54(4) eu, and $\Delta G^‡_{358\ K}$ = 28(3) kcal/mol. The activation entropy $\Delta S^‡$ is large negative, and its contribution ($-T\Delta S^‡$) to the activation free energy $\Delta G^‡_{358\ K}$ is more than twice that of the activation enthalpy $\Delta H^‡$. This perhaps reflects the following facts: (1) The reaction between **1** and $O_2$ is a dimolecular reaction. (2) Hexacoordinated **1** with two bulky guanidinate ligands is a highly crowded molecule, as its crystal structure revealed,[12x] making the metal center difficult to reach. Although heating does not favor the dimolecular reaction entropically, increased Zr−N vibrations at higher temperatures weaken the bonds and their stretching and bending modes provide opportunities for $O_2$ to attack the Zr center. Large negative $\Delta S^‡$ have been observed in associative reactions that follow second-order kinetics.[21h,23] The reaction of **1** with $O_2$ is autoxidation, and such reactions often have variable initiation periods.[6l,24] Although we did not observe such an effect in our studies, the autoxidation may have contributed to the relatively large errors in the kinetic plots and the small correlation coefficient $R^2$ value of 0.975 in the Eyring plot (Figure S15 in the SI).

We earlier found that the reactions of $M(NMe_2)_4$ (M = Zr, Hf) with $O_2$ at room temperature were fast,[7a] yielding overnight trinuclear complexes in Scheme 5. The presence of two guanidinate ligands in **1** significantly reduces the rate of its reaction with $O_2$, and prolonged heating at >80 °C is required to complete the reaction.

**Kinetic Studies of the Reaction of 1 with $O_2$ in the Presence of the Radical Initiator Azobis(isobutyronitrile) (AIBN).** $O_2$ is a diradical in the ground state, and many of its

**Scheme 7. Reactions of 1−3 with Water in Air; Species Observed by MS**

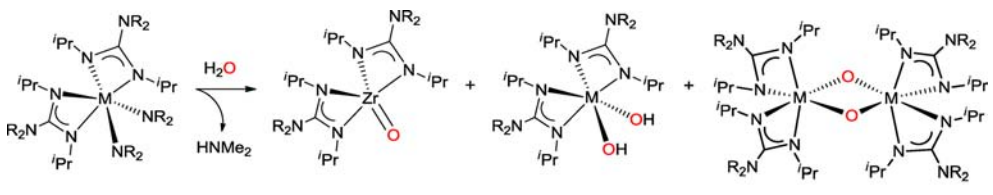


M = Zr; R = Me, **1**; Et, **3**
M = Hf; R = Me, **2**

R = Me, **10**; Et, **13**

M = Zr; R = Me, **11**; Et, **14**
M = Hf; R = Me, **12**

M = Zr; R = Me, **4**; Et, **6**
M = Hf; R = Me, **5**

**11 (14) → 10 (13) + $H_2O$**


dx.doi.org/10.1021/ic4016965 | Inorg. Chem. 2013, 52, 11409−11421

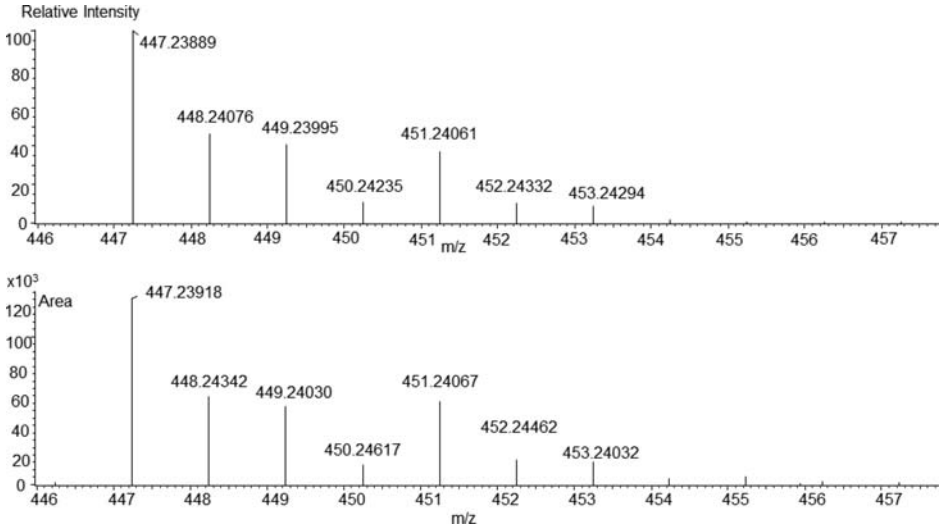


**Figure 2.** (top) Calculated and (bottom) observed MS for [**10** + $H^+$].

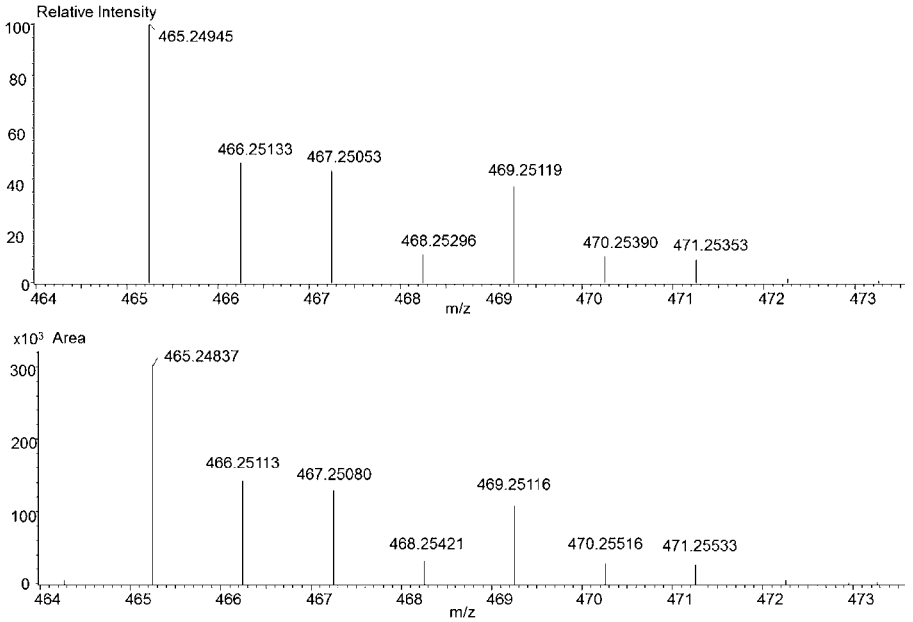


**Figure 3.** (top) Calculated and (bottom) observed MS for [**11** + $H^+$].

reactions are radical in nature. Because the reaction of **1** with $O_2$ is slow (Scheme 3), we studied the effect of the radical initiator AIBN.[61] AIBN, upon heating, decomposes to yield two radicals, as shown in Scheme 8. Kinetic studies of autoxidation has often been conducted using a radical initiator such as AIBN to provide reproducible reaction rates.[24] It has also been used to study the kinetics of the reaction between (bipy)$PdMe_2$ (bipy = 2,2′-bipyridine) with $O_2$ to give the methyl peroxide complex (bipy)PdMe(OOMe).[61] Kinetic studies were conducted in solutions containing AIBN and **1** in a 1:1 molar ratio in toluene-$d_8$ under 1 atm of $O_2$. The reaction at 65(1) °C was monitored and found to give the dimer **4**. Prior to this, a test reaction of **1** with AIBN was conducted, and the test showed that they did not react in the absence of $O_2$.

The kinetic plot (Figure S16 in the SI[16]) yields the observed rate constant of $8.584(3) \times 10^{-3}$ $min^{-1}$ for the reaction (in the presence of AIBN) at 65(1) °C. The half-life is 80.75(3) min. The predicted rate constant of the reaction (without AIBN) at 65(1) °C is $1.53 \times 10^{-3}$ $min^{-1}$,[16] and the half-life of the reaction between **1** and 1 atm of $O_2$ is expected to be 453(1) min. This reaction with AIBN is thus 5.6 times faster than that without the radical initiator. The results are consistent with the radical nature of the reactions between **1** and $O_2$.

**Reaction of $(Me_2N)_2Hf[^iPrNC(NMe_2)N^iPr]_2$ (2) with $O_2$ or $H_2O$.** Although zirconium and hafnium compounds often show similar reactivitivies, the reaction of $O_2$ with **2**, the hafnium analogue of **1**, was studied because the formation of $HfO_2$ as microelectronic materials from such reactions is of particular interest.

In a Young's NMR tube, a solution of **2** in benzene-$d_6$ under 1 atm of $O_2$ showed no reaction at room temperature. This solution was then heated at ca. 70 °C for 45 h, and the reaction was followed by $^1H$ NMR spectroscopy. Precipitation started right after the addition of $O_2$ and increased with heating of the reaction mixture. The NMR spectra (Figure S17 in the SI[16]) point to the formation of **16**, $HNMe_2$, the dimer $\{Hf(\mu\text{-}O)[^iPrNC(NMe_2)N^iPr]_2\}_2$ (**5**), and the polymer $\{Hf(\mu\text{-}O)[^iPrNC(NMe_2)N^iPr]_2\}_n$ (**8**). In the $^1H$ NMR spectrum


dx.doi.org/10.1021/ic4016965 | Inorg. Chem. 2013, 52, 11409−11421

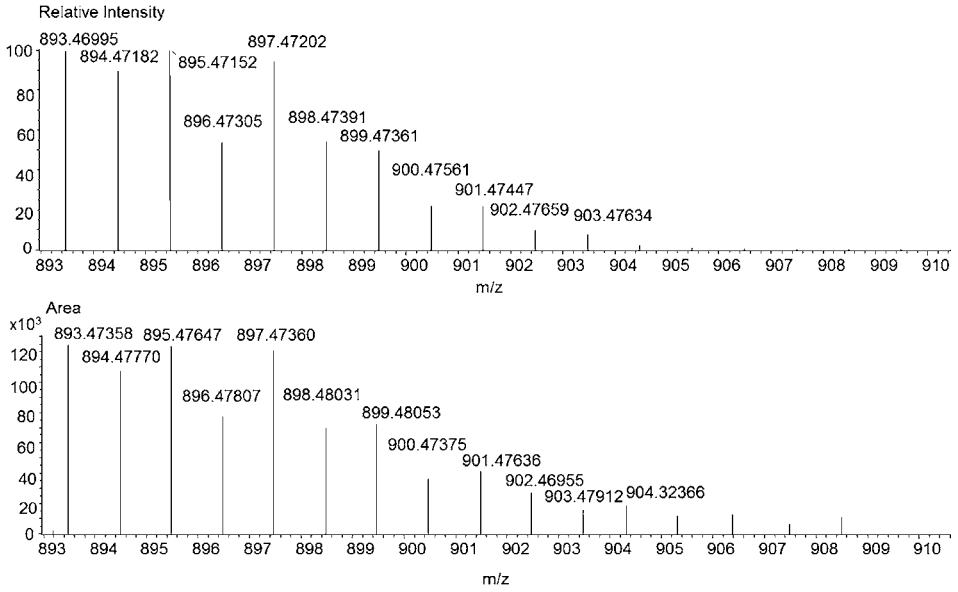


**Figure 4.** (top) Calculated and (bottom) observed MS for [**4** + $H^+$].

**Table 2. Rate Constants for the Reaction of 1 with $O_2$[a]**

| temperature | rate constant $k'$ ($min^{-1}$) |
|---|---|
| 353(1) | $2.925(4) \times 10^{-3}$ |
| 358(1) | $3.253(14) \times 10^{-3}$ |
| 363(1) | $3.67(11) \times 10^{-3}$ |
| 368(1) | $4.8(3) \times 10^{-3}$ |
| 373(1) | $5.84(3) \times 10^{-3}$ |
| 378(1) | $6.8(2) \times 10^{-3}$ |

[a]The total uncertainty $\delta k'/k'$ of 0.080 was calculated from $\delta k'_{ran}/k' = 0.063$ and $\Delta k'_{sys}/k' = 0.050$ for the measurements by NMR.

**Scheme 8. Thermal Decomposition of AIBN Giving Radicals and Initiation of Autoxidation of Substrates**

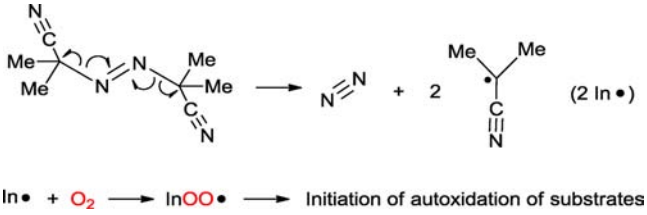


(Figure S17 in the SI,[16] top), two doublets were observed at 0.88 and 1.25 ppm for the CH*Me*$_2$ group. The singlet at 2.65 ppm and the multiplet at 3.31 ppm were assigned to the CN*Me*$_2$ and C*H*Me$_2$ atoms, respectively. In the $^{13}C\{^1H\}$ NMR spectrum (Figure S17 in the SI,[16] bottom), two peaks at 23.65 and 25.69 ppm are assigned to methyl groups in the isopropyl CH*Me*$_2$ moieties, and their *C*H groups are observed at 46.17 and 47.71 ppm. The peaks at 39.72 and 160.01 ppm are assigned to the methyl groups in the CN*Me*$_2$ moiety on the guanidinate [$^i$PrNC(NMe$_2$)N$^i$Pr]$^-$ ligand and its quaternary C atom, respectively. The IR spectrum of the insoluble product **8** (Figure S18 in the SI[16]) shows a strong peak at 1628 $cm^{-1}$, indicating the presence of the guanidinate ligand in the solid. These observations support the assignment of the solid as polymer **8**. The results here are similar to those of the zirconium analogue **1** and point to the reaction given in Scheme 3.

The reaction of **2** with $H_2O$ was found to be similar to that of its zirconium analogue **1** (Scheme 3), yielding HNMe$_2$, the dimer **5**, and the polymer **8** as well.

**MS Studies of the Reaction between 2 and $H_2O$ in Air.** Similar to its zirconium analogue, hafnium is an element with several stable isotopes [$^{174}$Hf, 0.16(1)%; $^{176}$Hf, 5.26(7)%; $^{177}$Hf, 18.60(9)%; $^{178}$Hf, 27.28(7)%; $^{179}$Hf, 13.62(2)%; $^{180}$Hf, 35.08(16)%]. MS spectra of hafnium compounds containing, for example, one and two Hf atoms thus each showed unique isotopic patterns. The MS studies here were performed similarly to those of its zirconium analogue **1**. Solid powders of **2** were kept under nitrogen gas until shortly before MS analysis. Molecules of **2** reacted with $H_2O$ in air, and transient products [M + $H^+$] were then analyzed by MS.

The calculated and observed MS spectra are given in Figures S19 and S20 in the SI.[16] They point to the reaction shown in Scheme 7 with formation of the dihydroxyl complex Hf(OH)$_2$[$^i$PrNC(NMe$_2$)N$^i$Pr]$_2$ (**12**) and the dimer **5**. The [M + $H^+$] peak for the dihydroxyl complex **12** was observed at *m*/*z* 551.43002 (calcd *m*/*z* 551.28615; Figure S19 in the SI[16]). For the dimer **5**, its [**5** + $H^+$] peak was observed at *m*/*z* 1067.73474, and the calculated peak was at *m*/*z* 1067.54659 (Figure S20 in the SI[16]).

**Reaction of 3 with $O_2$.** **3** is the diethylamide analogue of **1**.[12x] In addition to the NEt$_2$ ligands bound to the Zr atom, the guanidinate ligands also contain NEt$_2$ groups. The studies here, conducted on an NMR scale, offer a comparison with the reaction of **1** with $O_2$, and the results point to the reaction given in Scheme 3.

In a Young's NMR tube, the reaction of **3** with 1 atm of $O_2$ (2 equiv) initially conducted in benzene-$d_6$. No reaction was observed at room temperature over several days. At 75 °C, the reaction proceeded very slowly and the $^1$H NMR peaks corresponding to **3** decreased, and those corresponding to the dimer {Zr($\mu$-O)[$^i$PrNC(NEt$_2$)N$^i$Pr]$_2$}$_2$ (**6**) increased in intensity. After heating at 75 °C for 1 week, the volatiles were removed in vacuo and the residue was redissolved in toluene-$d_8$. To this solution was then added 1 atm of $O_2$, and the mixture was heated at 105 °C for 3 weeks. The $^1$H NMR peaks of **3** had disappeared completely.


dx.doi.org/10.1021/ic4016965 | Inorg. Chem. 2013, 52, 11409−11421

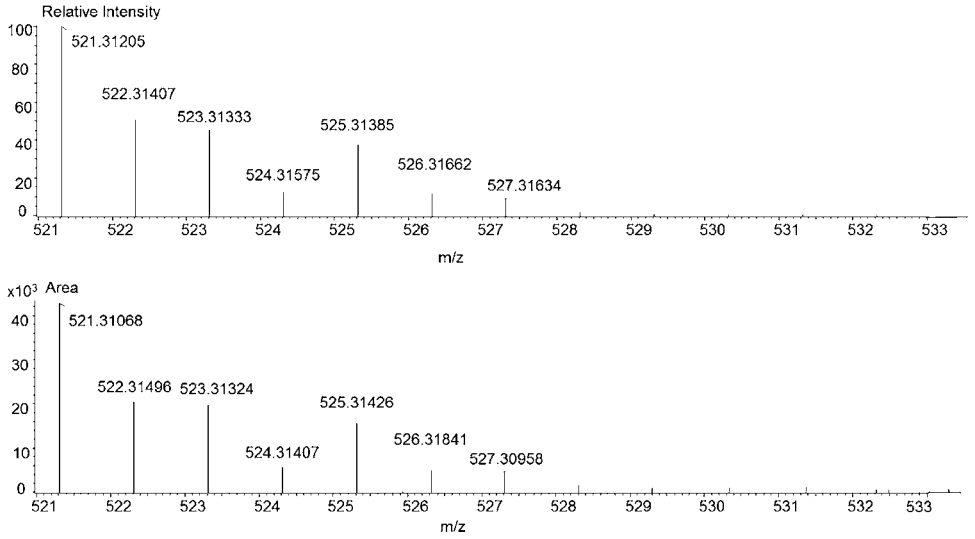


**Figure 5.** (top) Calculated and (bottom) observed MS for [**13** + $H^+$].

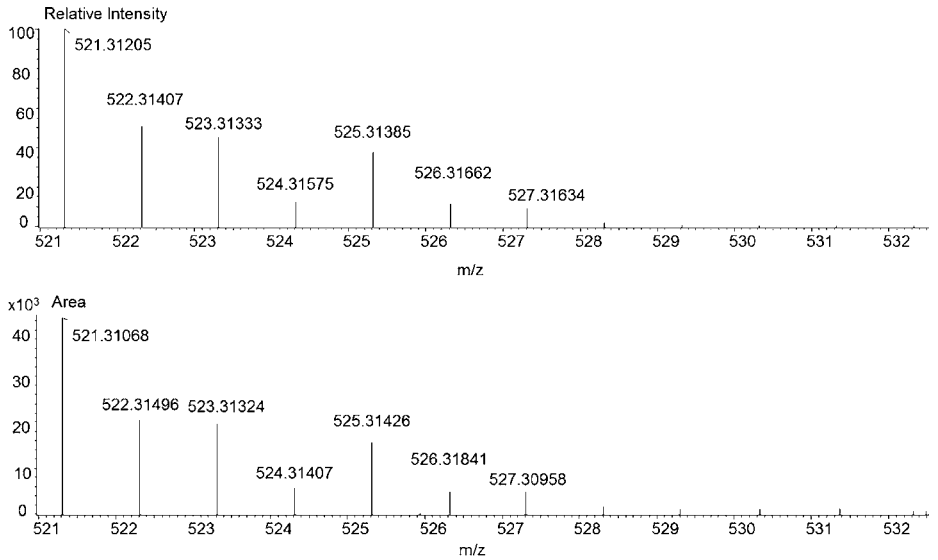


**Figure 6.** (top) Calculated and (bottom) observed MS for [**14** + $H^+$].

In $^1$H NMR spectrum (Figure S21 in the SI[16]), **6** showed two doublets at 0.92 and 1.19 ppm, which were assigned to the $CHMe_2$ groups. The $CN(CH_2CH_3)_2$ groups appeared as a triplet at 1.06 ppm. The quartet at 3.11 ppm was assigned to $CN(CH_2CH_3)_2$. Furthermore, the multiplets at 3.31 and 3.39 ppm were assigned to $CHMe_2$ protons. The main organic compound in this reaction mixture was $HNEt_2$, as confirmed by MS discussed below. The $^{13}C\{^1H\}$ NMR spectrum of **6** (Figure S22 in the SI[16]) showed peaks at 12.94 and 43.31 ppm for $CN(CH_2CH_3)_2$ and $CN(CH_2CH_3)_2$, respectively. The $CHMe_2$ groups were observed at 23.76 and 25.51 ppm, and the peaks at 46.20 and 47.73 ppm were assigned to $CHMe_2$. Finally, the $CNEt_2$ C atom was observed at 168.56 ppm. These assignments were confirmed by an HSQC experiment (Figure S23 in the SI[16]).

The precipitate, a light-yellow color, was found to be insoluble in organic solvents. Its IR spectrum (Figure S24 in the SI[16]) revealed a strong peak at 1622 $cm^{-1}$, suggesting the presence of the guanidinate ligand. These observations suggest that the insoluble solid is a polymeric product **9**, an analogue of **7** and **8**. Elemental analysis was consistent with **9**.

**MS Studies of the Reaction between 3 and $H_2O$ in Air.** These studies were performed similarly to those involving **1** and **2**. Molecules of **3** reacted with $H_2O$ in air, and transient products [M + $H^+$] (species + $H^+$) were then analyzed by MS. The calculated and observed MS spectra are given in Figures 5−8. They point to the reaction shown in Scheme 7. A [M + $H^+$] peak at $m/z$ 503.29885 was assigned to the oxo compound $Zr(=O)[^iPrNC(NEt_2)N^iPr]_2$ (**13**), and its calculated [M + $H^+$] peak was at $m/z$ 503.30149 (Figure 5). The [M + $H^+$] peak for the dihydroxyl $Zr(OH)_2[^iPrNC(NEt_2)N^iPr]_2$ (**14**) was observed at $m/z$ 521.30761 (calcd: $m/z$ 521.31205; Figure 6). For the dimer **6**, its [M + $H^+$] peak was observed at $m/z$ 1007.68461, and the calculated [M + $H^+$] peak was at $m/z$ 1007.59700 (Figure 7). In addition to these species, $\{(Et_2N)Zr[^iPrNC(NEt_2)N^iPr]_2\}^+$ (**15**) was also observed at $m/z$ 558.37429. Its calculated [M + $H^+$] peak was at $m/z$ 558.38007 (Figure 8).

**Reaction of 1 with 2,2,6,6-Tetramethyl-piperidin-1-yl)oxyl (TEMPO).** TEMPO is an oxygen-containing, stable radical. It has been used as both an oxidant[25] and a radical-trapping reagent.[26] The radical-trapping technique often refers


dx.doi.org/10.1021/ic4016965 | Inorg. Chem. 2013, 52, 11409−11421

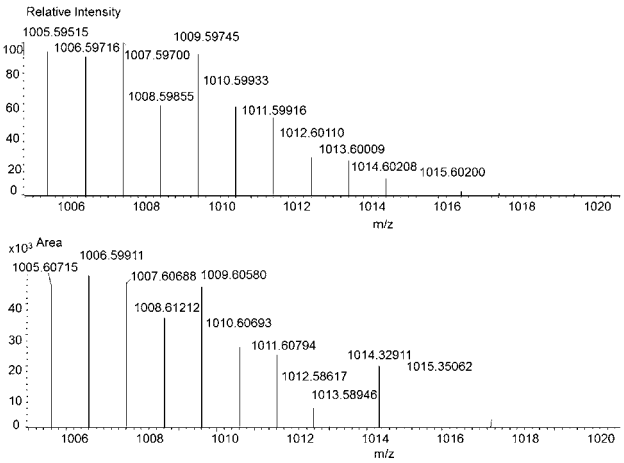


**Figure 7.** (top) Calculated and (bottom) observed MS for [**6** + $H^+$].

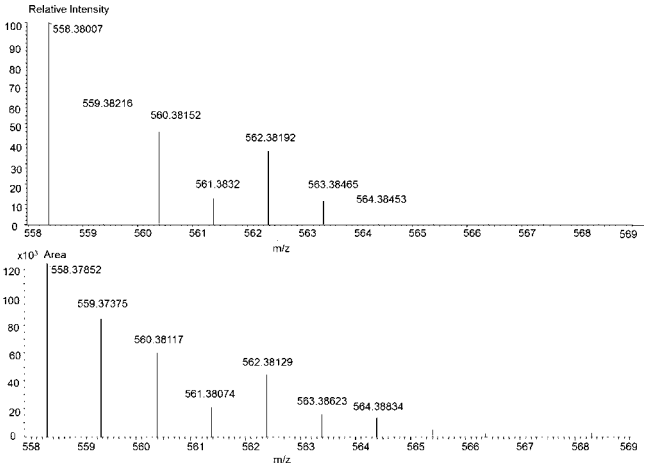


**Figure 8.** (top) Calculated and (bottom) observed MS of **15**.

to the use of a stable radical to react with a free radical R$^\bullet$ to give a *diamagnetic product* (Scheme 9). The diamagnetic product can then be analyzed to identify the radical R$^\bullet$.

**Scheme 9. Radical Trapping by TEMPO**

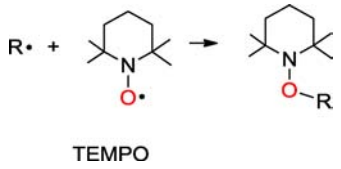


TEMPO

We have looked into whether, in the reaction of **1** with $O_2$ here, TEMPO acts as an oxidant or a radical-trapping reagent. TEMPO reacted with **1** (in the absence of $O_2$) to give the dimeric product **4** (Scheme 10 and Figures S25 and S26 in the SI[16]). GC−MS analysis of the volatiles from this reaction showed $HNMe_2$, **16**, and unreacted TEMPO as the main constituents. The formation of **4** here supports a radical pathway in the formation of **4**.

## ■ CONCLUSIONS

$O_2$ and $H_2O$ are two chemicals in air reacting with early-transition-metal compounds, often leading to their decomposition. They are also two primary oxygen sources in making metal oxide electronic materials. Our work shows that reactions of the amide guanidinate complexes here with $O_2$ or $H_2O$ remove the amide ligands, both yielding oxo dimers that, observed in the gas phase through MS, then convert into polymers using oxo bridges. In reactions with $H_2O$, several additional species, including dihydroxyl guanidinate complexes, were observed in MS.

The reactions of $O_2$ with the amide guanidinates are radical in nature. The guanidinate ligands significantly reduce the rates of reaction with $O_2$. Complex **3**, with the $NEt_2$-containing guanidinate and $NEt_2$ ligands, reacts with $O_2$ much more slowly than **1** and **2** with the $NMe_2$-containing guanidinate and $NMe_2$ ligands. The reactions of $H_2O$ with these amide guanidinate complexes are, however, fast even at room temperature. $H^+$ transfer from $H_2O$ to $MNR_2$ amide ligands is the primary pathway in the reactions of the guanidinate amide complexes with $H_2O$. The guanidinate ligands remain after the reactions with $O_2$ or $H_2O$ under the current reaction conditions. As a protecting group in the complexes, they offer opportunities to isolate or observe the products in the gas phase and in solution.

## ■ EXPERIMENTAL SECTION

All manipulations were performed under a dry nitrogen atmosphere with the use of either a drybox or standard Schlenk techniques. All solvents such as pentane, THF, and hexanes were dried over potassium/benzophenone, distilled, and stored under nitrogen. Benzene-$d_6$ and toluene-$d_8$ were dried over activated molecular sieves and stored under nitrogen. Toluene-$d_8$ was used in kinetic studies. NMR spectra were recorded on a Varian 500 MHz Fourier transform spectrometer unless otherwise noted and were referenced to solvents. Elemental analyses were conducted via Complete Analysis Laboratories, Inc., Parsippany, NJ. Solid-state NMR spectra were recorded on a solid-state Varian INOVA 400 MHz spectrometer. MS spectra were recorded on a JEOL AccuTOF DART mass spectrometer. To record IR spectra, solid samples were grounded with KBr, which had been dried at 100 °C and then pressed into pellets. IR spectra were recorded on a Varian 4100 Excalibur.

**Scheme 10. Reaction of 1 with TEMPO**

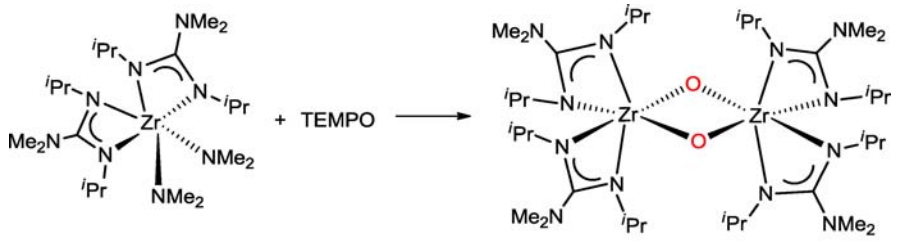


**1** **4**


dx.doi.org/10.1021/ic4016965 | *Inorg. Chem.* 2013, 52, 11409−11421

In the kinetic studies, at least two separate experiments performed for all temperatures gave the uncertainty. The *maximum* random uncertainty in the rate constants was combined with the estimated systematic uncertainty, ca. 5.0%. The total uncertainties in the rate constants were used in the Eyring plots[16] and error propagation calculations. The estimated uncertainty in the temperature measurements for an NMR probe and an oil bath was 1 K. The uncertainties in $\Delta H^{\ddagger}$ and $\Delta S^{\ddagger}$ were computed from the following error propagation formulas, which were derived by Girolami and co-workers from the Eyring equation $R \ln(kh/k_bT) = -\Delta H^{\ddagger}/T + \Delta S^{\ddagger}$.[27]

$$(\sigma\Delta H^{\ddagger})^2 = R^2 T_{max}{}^2 T_{min}{}^2/\Delta T^2\{(\sigma T/T)^2[(1 + T_{min}\Delta L/\Delta T)^2 + (1 + T_{max}\Delta L/\Delta T)^2] + 2(\sigma k/k)^2\} \quad (4)$$

$$(\sigma\Delta S^{\ddagger})^2 = R^2/\Delta T^2\{(\sigma T/T)^2[T_{max}{}^2(1 + T_{min}\Delta L/\Delta T)^2 + T_{min}{}^2(1 + T_{max}\Delta L/\Delta T)^2] + (\sigma k/k)^2 (T_{max}{}^2 + T_{min}{}^2)\} \quad (5)$$

where

$$\Delta L = [\ln(k_{max}/T_{max}) - \ln(k_{min}/T_{min})] \text{ and } \Delta T = T_{max} - T_{min}$$

**Reaction of 1 with $O_2$.** *NMR-Scale Reactions.* In a Young's NMR tube, **1** (38.7 mg, 0.0494 mmol) was dissolved in toluene-$d_8$. (The volume of the headspace in the Young's NMR tube was 2.4 mL.) Before $O_2$ was added, the solution was frozen in liquid nitrogen and nitrogen gas was removed in vacuo. $O_2$ (0.5 atm, 0.0494 mmol) was then added. $^1$H NMR spectra over a period of time showed no new peaks at room temperature, indicating no reaction of **1** with $O_2$. The Young's NMR tube was then heated at ca. 60 °C. The disappearance of **1** began, as revealed by the $^1$H NMR spectrum.

In a separate test, $O_2$ (1 atm, 0.123 mmol) was added to **1** (48.1 mg, 0.0614 mmol) in toluene-$d_8$. (The volume of the headspace in the Young's NMR tube was 3.0 mL.) $Si(SiMe_3)_4$ (5.0 mg) was used as an internal standard. The NMR tube was heated at 90 °C. After ca. 40 h, the reaction was quenched in ice water. The $^1$H NMR spectrum was recorded. The volatiles were removed in vacuo, and another $^1$H NMR spectrum of the residue was recorded. The spectra clearly showed the disappearance of **1** and appearance of new peaks corresponding to the oxo-bridged dimer **4**. The $^1$H NMR spectrum also revealed peaks corresponding to $HNMe_2$ (0.003 g, 6.23% yield based on NMR) and **16** (0.015 g, 31.2% yield based on NMR). The presence of $HNMe_2$ and **16** was confirmed with GC–MS. A white precipitate formed and was identified as the polymeric product **7** (0.028 g, 58.3% yield). The IR spectrum of **7** shows a strong peak at 1624 cm$^{-1}$.

The reaction of **1** with $O_2$ was repeated in benzene-$d_6$. $^1$H NMR of **4** (benzene-$d_6$, 499.7 MHz, 25 °C): $\delta$ 3.30 (m, 8H, C*H*Me$_2$), 2.64 (s, 24H, CN*Me*$_2$), 1.24 (d, 24H, CH*Me*$_2$, $^3J_{H-H}$ = 6.16 Hz), 0.88 (d, 24H, CH*Me*$_2$, $^3J_{H-H}$ = 6.39 Hz). $^{13}$C{$^1$H} NMR (benzene-$d_6$, 125 MHz, 25 °C): $\delta$ 168.97 (*C*NMe$_2$), 47.70 (*C*HMe$_2$), 46.16 (*C*HMe$_2$), 39.69 (CN*Me*$_2$), 25.70 (CH*Me*$_2$), 23.66 (CH*Me*$_2$).

*Reaction Conducted in a Schlenk Flask.* In another experiment, $O_2$ (1 atm, 1.895 mmol) was added to **1** (0.7427 g, 0.9472 mmol) in toluene in a Schlenk flask. The headspace of the Schlenk flask was 46.33 mL. The solution was heated at 90 °C for ca. 40 h. A white solid precipitated from the solution. Volatiles were removed in vacuo, and $Et_2O$ was added. The solution was concentrated in an attempt to grow crystals. No crystals could be isolated from the mixture. Removal of all of the volatiles yielded a white product of **7** (0.46 g, 62% isolated yield), which was insoluble in the solvents tested, including pentane, hexanes, benzene, $Et_2O$, THF, and toluene.

This reaction in toluene was repeated at 95 °C (**1**:$O_2$ = 1:2), 100 °C (**1**:$O_2$ = 1:2), and once with a continuous flow of $O_2$ at ca. 90 °C for 18 h. In all three instances, formation of the white insoluble solid **7** was observed, which was filtered off from the solution. The filtrate was then concentrated and left in a freezer for several days. Repeated attempts to grow crystals failed to yield crystalline materials.

**Reaction of 1 with Water.** *NMR-Scale Reaction.* Water in THF (20% v/v, 5.2 $\mu$L, 0.058 mmol) was added dropwise to **1** (15 mg, 0.029 mmol) in benzene-$d_6$ in a Young's NMR tube. The progress of the reaction was followed by $^1$H NMR spectroscopy, revealing formation of the oxo-bridged dimer **4** and $HNMe_2$.

*Reaction Conducted in a Schlenk Flask.* **1** (700 mg, 1.35 mmol) dissolved in toluene was cooled to −78 °C. Water (121 $\mu$L, 1.35 mmol) in a $H_2O$/THF mixture (20% v/v $H_2O$) at −78 °C was added dropwise to the solution of **1**. The solution was gradually warmed to room temperature. A large amount of white precipitate formed. Filtration and separation of the insoluble solid of **7** were performed (isolated 0.41 g, 59% yield). Attempts to grow crystals of the dimer **4** from the filtrate were unsuccessful. Solid-state $^{13}$C NMR of **7**: $\delta$ 159.17 (*C*NMe$_2$), 45.65 (*C*HMe$_2$), 39.93 (CN*Me*$_2$), 23.67 (CH*Me*$_2$). The IR spectrum of **7** showed a strong peak at 1625 cm$^{-1}$. Anal. Calcd for $C_{18}H_{40}N_6OZr$ (**7**): C, 48.28; H, 9.00; N, 18.77. Found: C, 48.15; H, 8.89; N, 18.68.

**Reaction of 2 with $O_2$.** $O_2$ (1 atm, 0.094 mmol) was added to **2** (21.8 mg, 0.036 mmol) in benzene-$d_6$ by the procedure described above for the reaction of **1** with $O_2$ in a Young's NMR tube. The solution was then heated at 70 °C. After 45 h, the peaks corresponding to **2** had disappeared, and the solution turned cloudy with solid precipitation. In addition to $HNMe_2$ and **16**, new peaks corresponding to the dimer product **5** were observed. $^1$H NMR of **5** (benzene-$d_6$, 499.7 MHz, 25 °C): $\delta$ 3.30 (m, 8H, C*H*Me$_2$), 2.65 (s, 24H, CN*Me*$_2$), 1.25 (d, 24H, CH*Me*$_2$, $^3J_{H-H}$ = 6.16 Hz), 0.88 (d, 24H, CH*Me*$_2$, $^3J_{H-H}$ = 6.4 Hz). $^{13}$C{$^1$H} NMR (benzene-$d_6$, 125 MHz, 25 °C): $\delta$ 160.01 (*C*NMe$_2$), 47.71 (*C*HMe$_2$), 46.16 (*C*HMe$_2$), 39.72 (CN*Me*$_2$), 25.69 (CH*Me*$_2$), 23.65 (CH*Me*$_2$). A white insoluble solid **8** (8.8 mg, 40% yield) was also formed that settled onto the bottom of the NMR tube. In the IR spectrum of **8**, a strong peak was observed at 1628 cm$^{-1}$.

**Reaction of 3 with $O_2$.** In an NMR-scale reaction, excess $O_2$ was added to **3** (31.2 mg, 0.0494 mmol) in benzene-$d_6$ in a Young's NMR tube. The solution was heated at 75 °C, but the $^1$H NMR peaks of **3** were still observed after several days of heating. The volatiles were then removed in vacuo, and toluene-$d_8$ was added as the solvent. The solution was then heated at 105 °C for ca. 3 weeks, after which **3** disappeared and peaks corresponding to the dimer **6** were observed.

In a large-scale test, to **3** (0.62 g, 0.98 mmol) in toluene in a Schlenk flask was added excess $O_2$. The reaction mixture was then heated at 105 °C for ca. 3 weeks, yielding a light-yellow solid precipitate. A small portion of the supernatant solution was removed from the Schlenk flask, and volatiles in the solution were removed. The $^1$H NMR spectrum of the residual solid from the supernatant solution revealed that **3** had completely converted. The light-yellow insoluble precipitate of $\{Zr(\mu\text{-}O)[^iPrNC(NEt_2)N^iPr]_2\}_n$ (**9**, isolated 0.41 g, 66% yield), an analogue of **7**, settled at the bottom of the Schlenk flask.

$^1$H NMR of **6** (benzene-$d_6$, 499.7 MHz, 25 °C): $\delta$ 3.30–3.39 (m, 8H, C*H*Me$_2$), 3.12 [q, 16H, CN(C*H*$_2$CH$_3$)$_2$, $^3J_{H-H}$ = 6.96 Hz], 1.18 (d, 24H, CH*Me*$_2$, $^3J_{H-H}$ = 6.12 Hz), 1.06 [t, 24H, CN(CH$_2$C*H*$_3$)$_2$, $^3J_{H-H}$ = 6.99 Hz], 0.92 (d, 24H, CH*Me*$_2$, $^3J_{H-H}$ = 6.37 Hz). $^{13}$C{$^1$H} NMR (benzene-$d_6$, 125 MHz, 25 °C): $\delta$ 168.56 (*C*NEt$_2$), 47.73 and 46.20 (*C*HMe$_2$), 43.31 [CN(*C*H$_2$CH$_3$)$_2$], 25.51 and 23.76 (CH*Me*$_2$), 12.94 [CN(CH$_2$*C*H$_3$)$_2$]. The IR spectral peak of the white insoluble solid **9** was observed at 1622 cm$^{-1}$. Anal. Calcd for $C_{22}H_{48}N_6OZr$ (**9**): C, 52.44; H, 9.60; N, 16.68. Found: C, 52.33; H, 9.47; N, 16.59.

**Kinetic Studies of the Reaction between 1 and $O_2$.** $MeSiPh_3$ (internal standard, 6.0 mg, 0.022 mmol) and **1** (20.0 mg, 0.0385 mmol) were dissolved in toluene-$d_8$ in a Young's NMR tube. A homemade setup (Figure S14 in the SI[16]) was used to provide a constant pressure of $O_2$ throughout the kinetic experiment. The NMR tube was then heated in an oil bath at the set temperature with a constant $O_2$ flow (1 atm).[16] At regular intervals, the NMR tube was removed from the oil bath and placed in ice water to quench the reaction. $^1$H NMR spectra were recorded. The ZrN*Me*$_2$ peak in **1** at 3.27 ppm was integrated with respect to the *Me*SiPh$_3$ peak at 0.72 ppm for each $^1$H NMR spectrum. These integrals were then plotted versus time (min). Kinetic studies were conducted at 80, 85, 90, 95, 100, 105, and 110 °C, and the test at each temperature was repeated at least once.


dx.doi.org/10.1021/ic4016965 | *Inorg. Chem.* 2013, 52, 11409–11421

## ■ ASSOCIATED CONTENT

### Supporting Information

Additional results and discussion, NMR and IR spectra, kinetic plots, an experimental apparatus for kinetic studies of the reaction between **1** and $O_2$, and an additional experimental section. This material is available free of charge via the Internet at http://pubs.acs.org.

## ■ AUTHOR INFORMATION


### Corresponding Author

*E-mail: xue@utk.edu.


### Notes

The authors declare no competing financial interest.

## ■ ACKNOWLEDGMENTS

The work is supported by the U.S. National Science Foundation (Grant CHE-1012173). The authors thank Stephen C. Gibson and Dr. Liguo Song for assistance with MS studies and Matthew D. Dembo for help with the solid-state NMR work.

## ■ DEDICATION

†This paper is dedicated to Professor Xiao-Zeng You on the occasion of his 80th birthday.

## ■ REFERENCES


(1) (a) Tilley, T. D. *Organometallics* **1985**, *4*, 1452. (b) Blackburn, T. F.; Labinger, J. A.; Schwartz, J. *Tetrahedron Lett.* **1975**, *16*, 3041. (c) Lubben, T. V.; Wolczanski, P. T. *J. Am. Chem. Soc.* **1987**, *109*, 424. (d) Wang, R.; Folting, K.; Huffman, J. C.; Chamberlain, L. R.; Rothwell, I. P. *Inorg. Chim. Acta* **1986**, *120*, 81. (e) Gibson, V. C.; Redshaw, C.; Walker, G. L. P.; Howard, J. A. K.; Hoy, V. J.; Cole, J. M.; Kuzmina, L. G.; De Silva, D. S. *J. Chem. Soc., Dalton Trans.* **1999**, 161. (f) Schaverien, C. J.; Orpen, A. G. *Inorg. Chem.* **1991**, *30*, 4968. (g) Liu, X.; Cui, D. *Dalton Trans.* **2008**, 3747. (h) Van Asselt, A.; Santarsiero, B. D.; Bercaw, J. E. *J. Am. Chem. Soc.* **1986**, *108*, 8291. (i) Kim, S. J.; Choi, D. W.; Lee, Y. J.; Chae, B. H.; Ko, J. J.; Kang, S. O. *Organometallics* **2004**, *23*, 559. (j) Morris, A. M.; Pierpont, C. G.; Finke, R. G. *Inorg. Chem.* **2009**, *48*, 3496. (k) Adam, W.; Putterlik, J.; Schuhmann, R. M.; Sundermeyer, J. *Organometallics* **1996**, *15*, 4586. (l) Vetter, W. M.; Sen, A. *Organometallics* **1991**, *10*, 244. (m) Van Asselt, A.; Trimmer, M. S.; Henling, L. M.; Bercaw, J. E. *J. Am. Chem. Soc.* **1988**, *110*, 8254. (n) Boro, B. J.; Lansing, R.; Goldberg, K. I.; Kemp, R. A. *Inorg. Chem. Commun.* **2011**, *14*, 531.

(2) Stanciu, C.; Jones, M. E.; Fanwick, P. E.; Abu-Omar, M. M. *J. Am. Chem. Soc.* **2007**, *129*, 12400.

(3) Lu, F.; Zarkesh, R. A.; Heyduk, A. F. *Eur. J. Inorg. Chem.* **2012**, 467.

(4) Chisholm, M. H.; Hammond, C. E.; Huffman, J. C. *J. Chem. Soc., Chem. Commun.* **1987**, 1423.

(5) Brindley, P. B.; Hodgson, J. C. *J. Organomet. Chem.* **1974**, *65*, 57.

(6) For studies of the reactions between $O_2$ and late-transition-metal complexes, see, for example: (a) Campbell, A. N.; Stahl, S. S. *Acc. Chem. Res.* **2012**, *45*, 851. (b) Theopold, K. H.; Reinaud, O. M.; Blanchard, S.; Leelasubeharoen, S.; Hess, A.; Thyagarajan, S. *ACS Symp. Ser.* **2002**, *823*, 75. (c) Que, L.; Tolman, W. B. *Nature* **2008**, *455*, 333. (d) Himes, R. A.; Karlin, K. D. *Curr. Top. Chem. Biol.* **2009**, *13*, 119. (e) Shook, R. L.; Borovik, A. S. *Chem. Commun.* **2008**, 6095. (f) Sheldon, R. A. In *Biomimetic Oxidations Catalyzed by Transition Metal Complexes*; Meunier, B., Ed.; Imperial College Press: London, 2000; pp 613−662. (g) Metal−Dioxygen Complexes: A Perspective. Special Issue: *Chem. Rev.* **1994**, *94* (3), 567−856. (h) Monillas, W. H.; Yap, G. P. A.; MacAdams, L. A.; Theopold, K. H. *J. Am. Chem. Soc.* **2007**, *129*, 8090. (i) McQuilken, A. C.; Jiang, Y.; Siegler, M. A.; Goldberg, D. P. *J. Am. Chem. Soc.* **2012**, *134*, 8758. (j) Prokop, K. A.; Goldberg, D. P. *J. Am. Chem. Soc.* **2012**, *134*, 8014. (k) Scheuermann, M. L.; Fekl, U.; Kaminsky, W.; Goldberg, K. I. *Organometallics* **2010**, *29*, 4749. (l) Boisvert, L.; Denney, M. C.; Kloek Hanson, S.; Goldberg, K. I. *J. Am. Chem. Soc.* **2009**, *131*, 15802. and references cited therein. (m) Khusnutdinova, J. R.; Rath, N. P.; Mirica, L. M. *J. Am. Chem. Soc.* **2012**, *134*, 2414. (n) Nguyen, K. T.; Rath, S. P.; Latos-Grazynski, L.; Olmstead, M. M.; Balch, A. L. *J. Am. Chem. Soc.* **2004**, *126*, 6210. (o) Maury, J.; Feray, L.; Bazin, S.; Clement, J.-L.; Marque, S. R. A.; Siri, D.; Bertrand, M. P. *Chem.—Eur. J.* **2011**, *17*, 1586. (p) Lewinski, J.; Koscielski, M.; Suwala, K.; Justyniak, I. *Angew. Chem., Int. Ed.* **2009**, *48*, 7017. (q) Mukherjee, D.; Ellern, A.; Sadow, A. D. *J. Am. Chem. Soc.* **2012**, *134*, 13018. (r) Jana, S.; Berger, R. J. F.; Fröhlich, R.; Pape, T.; Mitzel, N. W. *Inorg. Chem.* **2007**, *46*, 4293. (s) Lee, C.-M.; Chuo, C.-H.; Chen, C.-H.; Hu, C.-C.; Chiang, M.-H.; Tseng, Y.-J.; Hu, C.-H.; Lee, G.-H. *Angew. Chem., Int. Ed.* **2012**, *51*, 5427. (t) Kelley, M. R.; Rohde, J.-U. *Chem. Commun.* **2012**, *48*, 2876. (u) Brown, S. N.; Mayer, J. M. *Inorg. Chem.* **1992**, *31*, 4091. (v) Parkin, G.; Bercaw, J. E. *J. Am. Chem. Soc.* **1989**, *111*, 391.

(7) (a) Wang, R.; Zhang, X.; Chen, S.; Yu, X.; Wang, C.; Beach, D. B.; Wu, Y.; Xue, Z. *J. Am. Chem. Soc.* **2005**, *127*, 5204. (b) Chen, S.; Zhang, X.; Yu, X.; Qiu, H.; Yap, G. P. A.; Guzei, I. A.; Lin, Z.; Wu, Y.; Xue, Z. *J. Am. Chem. Soc.* **2007**, *129*, 14408. (c) Chen, S.-J.; Zhang, X.-H.; Lin, Z.; Wu, Y.-D.; Xue, Z.-L. *Sci. China Chem.* **2009**, *52*, 1723. (d) Chen, S.-J.; Yap, G. P. A.; Xue, Z.-L. *Sci. China Chem.* **2009**, *52*, 1583. (e) Chen, S.; Zhang, J.; Yu, X.; Bu, X.; Chen, X.; Xue, Z. *Inorg. Chem.* **2010**, *49*, 4017. (f) Chen, T.-N.; Zhang, X.-H.; Wang, C.-S.; Chen, S.-J.; Wu, Z.-Z.; Li, L.-T.; Sorasaenee, K. R.; Diminnie, J. B.; Pan, H.-J.; Guzei, I. A.; Rheingold, A. L.; Wu, Y.-D.; Xue, Z.-L. *Organometallics* **2005**, *24*, 1214. (g) Qiu, H.; Chen, S.-J.; Wang, C.-S.; Wu, Y.-D.; Guzei, I. A.; Chen, X.-T.; Xue, Z.-L. *Inorg. Chem.* **2009**, *48*, 3073. (h) Yu, X.; Chen, X.-T.; Xue, Z.-L. *Organometallics* **2009**, *28*, 6642. (i) Chen, S.-J.; Xue, Z.-L. *Organometallics* **2010**, *29*, 5579. (j) Wu, Z.; Cai, H.; Yu, X.-H.; Blanton, J. R.; Diminnie, J. B.; Pan, H.-J.; Xue, Z.-L. *Organometallics* **2002**, *21*, 3973.

(8) (a) Miller, J. B.; Schwartz, J.; Bernasek, S. L. *J. Am. Chem. Soc.* **1984**, *115*, 8239. (b) Feinstein-Jaffe, I.; Gibson, D.; Lippard, S. J.; Schrock, R. R.; Spool, A. *J. Am. Chem. Soc.* **1984**, *106*, 6305. (c) Schoettel, G.; Kress, J.; Fischer, J.; Osborn, J. A. *J. Chem. Soc., Figure 2a - The label [M-2H]1-. at the far right side of the figure should not be split over two lines.Chem. Commun.* **1988**, 914. (d) Legzdins, P.; Phillips, E. C.; Rettig, S. J.; Sanchez, L.; Trotter, J.; Yee, V. C. *Organometallics* **1988**, *7*, 1877. (e) Gamble, A. S.; Boncella, J. M. *Organometallics* **1993**, *12*, 2814. (f) Guzyr, O. I.; Prust, J.; Roesky, H. W.; Lehmann, C.; Teichert, M.; Cimpoesu, F. *Organometallics* **2000**, *19*, 1549. (g) Yoon, M.; Tyler, D. R. *Chem. Commun.* **1997**, 639. (h) Chen, S.-J.; Abbott, J. K. C.; Steren, C. A.; Xue, Z.-L. *J. Cluster Sci.* **2010**, *21*, 325. (i) Chen, S.-J.; Cai, H.; Xue, Z.-L. *Organometallics* **2009**, *28*, 167. (j) Dougan, B. A.; Xue, Z.-L. *Sci. China Chem.* **2011**, *54*, 1903.

(9) (a) Robertson, J. *Rep. Prog. Phys.* **2006**, *69*, 327. (b) Jones, A. C.; Aspinall, H. C.; Chalker, P. R.; Potter, R. J.; Kukli, K.; Rahtu, A.; Ritala, M.; Leskelae, M. *J. Mater. Chem.* **2004**, *14*, 3101. (c) Arghavani, R.; Miner, G.; Agustin, M. *Semicond. Int.* **2007**, *30* (32−34), 36−38.

(10) For CVD of metal oxides using $O_2$, see, for example: (a) Son, K.-A.; Mao, A. Y.; Sun, Y.-M.; Kim, B. Y.; Liu, F.; Kamath, A.; White, J. M.; Kwong, D. L.; Roberts, D. A.; Vrtis, R. N. *Appl. Phys. Lett.* **1998**, *72*, 1187. (b) Niimi, H.; Johnson, R. S.; Lucovsky, G.; Massoud, H. Z. *Proc. Electrochem. Soc.* **2000**, *2000−2*, 487. (c) Eichler, J. F.; Just, O.; Rees, W. S., Jr. *J. Mater. Chem.* **2004**, *14*, 3139. (d) Takahashi, K.; Funakubo, H.; Hino, S.; Nakayama, M.; Ohashi, N.; Kiguchi, T.; Tokumitsu, E. *J. Mater. Res.* **2004**, *19*, 584. (e) Ogura, A.; Ito, K.; Ohshita, Y.; Ishikawa, M.; Machida, H. *Thin Solid Films* **2003**, *441*, 161. (f) Rodriguez-Reyes, J. C. F.; Teplyakov, A. V. *J. Appl. Phys.* **2008**, *104*, 084907/1. (g) Ohshita, Y.; Ogura, A.; Ishikawa, M.; Kada, T.; Machida, H. *Jpn. J. Appl. Phys. 2* **2003**, *42*, L578. (h) Matero, R.; Ritala, M.; Leskelae, M.; Sajavaara, T.; Jones, A. C.; Roberts, J. L. *Chem. Mater.* **2004**, *16*, 5630. (i) Kan, B.-C.; Boo, J.-H.; Lee, I.; Zaera, F. *J. Phys. Chem. A* **2009**, *113*, 3946. (j) Hausmann, D. M.; de Rouffignac, P.; Smith, A.; Gordon, R.; Monsma, D. *Thin Solid Films* **2003**, *443*, 1. (k) Meiere, S. H.; Peck, J.; Litwin, M. *ECS Trans.* **2006**, *1*, 103.

(l) Chen, T.; Cameron, T. M.; Nguyen, S. D.; Stauf, G. T.; Peters, D. W.; Maylott, L.; Li, W.; Xu, C.; Roeder, J. F.; Hendrix, B. C.; Hilgarth, M.; Niinisto, J.; Kukli, K.; Ritala, M.; Leskela, M. *ECS Trans.* **2008**, *16*, 87. (m) Lee, S.; Kim, W.-G.; Rhee, S.-W.; Yong, K. *J. Electrochem. Soc.* **2008**, *155*, H92. (n) Schaeffer, J.; Edwards, N. V.; Liu, R.; Roan, D.; Hradsky, B.; Gregory, R.; Kulik, J.; Duda, E.; Contreras, L.; Christiansen, J.; Zollner, S.; Tobin, P.; Nguyen, B.-Y.; Nieh, R.; Ramon, M.; Rao, R.; Hegde, R.; Rai, R.; Baker, J.; Voight, S. *J. Electrochem. Soc.* **2003**, *150*, F67. (o) Woods, J. B.; Beach, D. B.; Nygren, C. L.; Xue, Z.-L. *Chem. Vap. Deposition* **2005**, *11*, 289. (p) Lehn, J.-S.; Javed, S.; Hoffman, D. M. *Chem. Vap. Deposition* **2006**, *12*, 280. (q) Chiu, H.-T.; Wang, C.-N.; Chuang, S.-H. *Chem. Vap. Deposition* **2000**, *6*, 223. (r) Wiedmann, M. K.; Heeg, M. J.; Winter, C. H. *Inorg. Chem.* **2009**, *48*, 5382.

(11) For CVD of metal oxides using water, see, for example: (a) Dezelah, C. L., IV; Niinisto, J.; Kukli, K.; Munnik, F.; Lu, J.; Ritala, M.; Leskela, M.; Niinisto, L. *Chem. Vap. Deposition* **2008**, *14*, 358. (b) Dezelah, C. L., IV; El-Kadri, O. M.; Szilagyi, I. M.; Campbell, J. M.; Arstila, K.; Niinist', L.; Winter, C. H. *J. Am. Chem. Soc.* **2006**, *128*, 9638. (c) Majumder, P.; Jursich, G.; Takoudis, C. *J. Appl. Phys.* **2009**, *105*, 104106/1. (d) Consiglio, S.; Clark, R. D.; Nakamura, G.; Wajda, C. S.; Leusink, G. J. *J. Vacuum Sci. Technol., A* **2012**, *30*, 01A119/1. (e) Tao, Q.; Kueltzo, A.; Singh, M.; Jursich, G.; Takoudis, C. G. *J. Electrochem. Soc.* **2011**, *158*, G27. (f) Shi, X.; Tielens, H.; Takeoka, S.; Nakabayashi, T.; Nyns, L.; Adelmann, C.; Delabie, A.; Schram, T.; Ragnarsson, L.; Schaekers, M.; Date, L.; Schreutelkamp, R.; Van Elshocht, S. *J. Electrochem. Soc.* **2011**, *158*, H69.

(12) For the studies of guanidinate complexes as CVD/ALD precursors, see, for example: (a) Wiedmann, M. K.; Heeg, M. J.; Winter, C. H. *Inorg. Chem.* **2009**, *48*, 5382. (b) Edelmann, F. T. *Chem. Soc. Rev.* **2009**, *38*, 2253. (c) Xu, K.; Milanov, A. P.; Parala, H.; Wenger, C.; Baristiran-Kaynak, C.; Lakribssi, K.; Toader, T.; Bock, C.; Rogalla, D.; Becker, H.-W.; Kunze, U.; Devi, A. *Chem. Vap. Deposition* **2012**, *18*, 27. (d) Thiede, T. B.; Krasnopolski, M.; Milanov, A. P.; de los Arcos, T.; Ney, A.; Becker, H.-W.; Rogalla, D.; Winter, J.; Devi, A.; Fischer, R. A. *Chem. Mater.* **2011**, *23*, 1430. (e) Baunemann, A.; Rische, D.; Milanov, A.; Kim, Y.; Winter, M.; Gemel, C.; Fischer, R. A. *Dalton Trans.* **2005**, 3051. (f) Hubert-Pfalzgraf, L. G.; Decams, J.-M.; Daniele, S. *J. Phys. IV* **1999**, *9*, 953. (g) Carmalt, C. J.; Newport, A. C.; O'Neill, S. A.; Parkin, I. P.; White, A. J. P.; Williams, D. J. *Inorg. Chem.* **2005**, *44*, 615. (h) Xu, K.; Milanov, A. P.; Winter, M.; Barreca, D.; Gasparotto, A.; Becker, H.-W.; Devi, A. *Eur. J. Inorg. Chem.* **2010**, 1679. (i) Whitehorne, T. J. J.; Coyle, J. P.; Mahmood, A.; Monillas, W. H.; Yap, G. P. A.; Barry, S. T. *Eur. J. Inorg. Chem.* **2011**, 3240. (j) Baunemann, A.; Winter, M.; Csapek, K.; Gemel, C.; Fischer, R. A. *Eur. J. Inorg. Chem.* **2006**, 4665. (k) Baunemann, A.; Bekermann, D.; Thiede, T. B.; Parala, H.; Winter, M.; Gemel, C.; Fischer, R. A. *Dalton Trans.* **2008**, 3715. (l) Milanov, A.; Bhakta, R.; Baunemann, A.; Becker, H.; Thomas, R.; Ehrhart, P.; Winter, M.; Devi, A. *Inorg. Chem.* **2006**, *45*, 11008. (m) Eleter, M.; Daniele, S.; Brize, V.; Dubourdieu, C.; Lachaud, C.; Blasco, N.; Pinchart, A. *ECS Trans.* **2009**, *25* (8, EuroCVD 17/CVD 17), 151. (n) Carmalt, C. J.; Newport, A. C.; O'Neill, S. A.; Parkin, I. P.; White, A. J. P.; Williams, D. J. *Inorg. Chem.* **2005**, *44*, 615. (o) Devi, A.; Bhakta, R.; Milanov, A.; Hellwig, M.; Barreca, D.; Tondello, E.; Thomas, R.; Ehrhart, P.; Winter, M.; Fischer, R. *Dalton Trans.* **2007**, 1671. (p) Chen, T.; Xu, C.; Baum, T. H.; Stauf, G. T.; Roeder, J. F.; DiPasquale, A. G.; Rheingold, A. L. *Chem. Mater.* **2010**, *22*, 27. (q) Coyle, J. P.; Monillas, W. H.; Yap, G. P. A.; Barry, S. T. *Inorg. Chem.* **2008**, *47*, 683. (r) Potts, S. E.; Carmalt, C. J.; Blackman, C. S.; Abou-Chahine, F.; Pugh, D.; Davies, H. O. *Organometallics* **2009**, *28*, 1838. (s) Chen, T.; Hunks, W.; Chen, P. S.; Stauf, G. T.; Cameron, T. M.; Xu, C.; Di Pasquale, A. G.; Rheingold, A. L. *Eur. J. Inorg. Chem.* **2009**, 2047. (t) Eleter, M.; Hubert-Pfalzgraf, L. G.; Daniele, S.; Pilet, G.; Tinant, B. *Polyhedron* **2010**, *29*, 2522. (u) Milanov, A. P.; Xu, K.; Laha, A.; Bugiel, E.; Ranjith, R.; Schwendt, D.; Osten, H. J.; Parala, H.; Fischer, R. A.; Devi, A. *J. Am. Chem. Soc.* **2010**, *132*, 36. (v) Barry, S. T.; Gordon, P. G.; Ward, M. J.; Heikkila, M. J.; Monillas, W. H.; Yap, G. P. A.; Ritala, M.; Leskelae, M. *Dalton Trans.* **2011**, *40*, 9425. (w) Wilder, C. B.; Reitfort, L. L.; Abboud, K. A.; McElwee-White, L. *Inorg. Chem.* **2006**, *45*, 263. (x) Banerjee, M.; Srinivasan, N. B.; Zhu, H.; Kim, S. J.; Xu, K.; Winter, M.; Becker, H.-W.; Rogalla, D.; de los Arcos, T.; Bekermann, D.; Barreca, D.; Fischer, R. A.; Devi, A. *Cryst. Growth Des.* **2012**, *12*, 5079. (y) Blanquart, T.; Niinisto, J.; Aslam, N.; Banerjee, M.; Tomczak, Y.; Gavagnin, M.; Longo, V.; Puukilainen, E.; Wanzenboeck, H. D.; Kessels, W. M. M.; Devi, A.; Hoffmann-Eifert, S.; Ritala, M.; Leskela, M. *Chem. Mater.* **2013**, *25*, 3088. (z) Kim, S. J.; Xu, K.; Parala, H.; Beranek, R.; Bledowski, M.; Sliozberg, K.; Becker, H.-W.; Rogalla, D.; Barreca, D.; Maccato, C.; Sada, C.; Schuhmann, W.; Fischer, R. A.; Devi, A. *Chem. Vap. Deposition* **2013**, *19*, 45.

(13) For reviews on guanidinate complexes, see, for example, the following: (a) Bailey, P. J.; Pace, S. *Coord. Chem. Rev.* **2001**, *214*, 91. (b) Edelmann, F. T. *Adv. Organomet. Chem.* **2008**, *57*, 183. (c) Zhang, W.-X.; Hou, Z. *Org. Biomol. Chem.* **2008**, *6*, 1720. (d) Jones, C. *Coord. Chem. Rev.* **2010**, *254*, 1273. (e) Edelmann, F. T. *Struct. Bonding (Berlin)* **2010**, *137* (Molecular Catalysis of Rare-Earth Elements), 109. (f) Li, T.; Jenter, J.; Roesky, P. W. *Struct. Bonding (Berlin)* **2010**, *137*, 165. (g) Trifonov, A. A. *Coord. Chem. Rev.* **2010**, *254*, 1327. (h) Barry, S. T. *Coord. Chem. Rev.* **2013**, http://dx.doi.org/10.1016/j.ccr.2013.03.015. (i) Marchand, P.; Carmalt, C. J. *Coord. Chem. Rev.* **2013**, http://dx.doi.org/10.1016/j.ccr.2013.01.030.

(14) (a) Chandra, G.; Jenkins, A. D.; Lappert, M. F.; Srivastava, R. C. *J. Chem. Soc. A* **1970**, 2550. (b) Aeilts, S. L.; Coles, M. P.; Swenson, D. C.; Jordan, R. F.; Young, V. G. *Organometallics* **1998**, *17*, 3265. (c) Tin, M. K. T.; Yap, G. P. A.; Richeson, D. S. *Inorg. Chem.* **1998**, *37*, 6728. (d) Decams, J. M.; Hubert-Pfalzgraf, L. G.; Vaissermann, J. *Polyhedron* **1999**, *18*, 2885. (e) Wood, D.; Yap, G. P. A.; Richeson, D. S. *Inorg. Chem.* **1999**, *38*, 5788. (f) Giesbrecht, G. R.; Whitener, G. D.; Arnold, J. *Organometallics* **2000**, *19*, 2809. (g) Bailey, P. J.; Grant, K. J.; Mitchell, L. A.; Pace, S.; Parkin, A.; Parsons, S. *Dalton Trans.* **2000**, 1887. (h) Duncan, A. P.; Mullins, S. M.; Arnold, J.; Bergman, R. G. *Organometallics* **2001**, *20*, 1808. (i) Soria, D. B.; Grundy, J.; Coles, M. P.; Hitchcock, P. B. *Polyhedron* **2003**, *22*, 2731. (j) Cotton, F. A.; Hillard, E. A.; Murillo, C. A.; Wang, X. *Inorg. Chem.* **2003**, *42*, 6063. (k) Pang, X.-A.; Yao, Y.-M.; Wang, J.-F.; Sheng, H.-T.; Zhang, Y.; Shen, Q. *Chin. J. Chem.* **2005**, *23*, 1193. (l) Guiducci, A. E.; Boyd, C. L.; Mountford, P. *Organometallics* **2006**, *25*, 1167. (m) Hirotsu, M.; Fontaine, P. P.; Zavalij, P. Y.; Sita, L. R. *J. Am. Chem. Soc.* **2007**, *129*, 12690. (n) Shen, H.; Chan, H.-S.; Xie, Z. *J. Am. Chem. Soc.* **2007**, *129*, 12934. (o) Zhou, M.; Zhang, S.; Tong, H.; Sun, W.-H.; Liu, D. *Inorg. Chem. Commun.* **2007**, *10*, 1262. (p) Gott, A. L.; Clarkson, G. J.; Deeth, R. J.; Hammond, M. L.; Morton, C.; Scott, P. *Dalton Trans.* **2008**, 2983. (q) Cotton, F. A.; Ibragimov, S. A.; Murillo, C. A.; Poplaukhin, P. V.; Zhao, Q. *J. Mol. Struct.* **2008**, *890*, 3. (r) Ren, S.; Deng, L.; Chan, H.-S.; Xie, Z. *Organometallics* **2009**, *28*, 5749. (s) Wasslen, Y. A.; Tois, E.; Haukka, S.; Kreisel, K. A.; Yap, G. P. A.; Halls, M. D.; Barry, S. T. *Inorg. Chem.* **2010**, *49*, 1976. (t) Maddox, A. F.; Erickson, K. A.; Tanski, J. M.; Waterman, R. *Chem. Commun.* **2011**, *47*, 11769. (u) Yonke, B. L.; Keane, A. J.; Zavalij, P. Y.; Sita, L. R. *Organometallics* **2012**, *31*, 345. (v) Elorriaga, D.; Carrillo-Hermosilla, F.; Antinolo, A.; Lopez-Solera, I.; Menot, B.; Fernandez-Galan, R.; Villasenor, E.; Otero, A. *Organometallics* **2012**, *31*, 1840. (w) Fernandez-Galan, R.; Antinolo, A.; Carrillo-Hermosilla, F.; Lopez-Solera, I.; Otero, A.; Serrano-Laguna, A.; Villasenor, E. *J. Organomet. Chem.* **2012**, *711*, 35. (x) Jones, C.; Schulten, C.; Nembenna, S.; Stasch, A. *J. Chem. Crystallogr.* **2012**, *42*, 866. (y) Fernandez-Galan, R.; Antinolo, A.; Carrillo-Hermosilla, F.; Lopez-Solera, I.; Otero, A.; Serrano-Laguna, A.; Villasenor, E. *Organometallics* **2012**, *31*, 8360. (z) Elorriaga, D.; Carrillo-Hermosilla, F.; Antinolo, A.; Suarez, F. J.; Lopez-Solera, I.; Fernandez-Galan, R.; Villasenor, E. *Dalton Trans.* **2013**, *42*, 8223.

(15) For lanthanide guanidinate complexes, see, for example, the following: (a) Zhou, Y.; Yap, G. P. A.; Richeson, D. S. *Organometallics* **1998**, *17*, 4387. (b) Luo, Y.; Yao, Y.; Shen, Q.; Yu, K.; Weng, L. *Eur. J. Inorg. Chem.* **2003**, 318. (c) Zhang, J.; Cai, R.; Weng, L.; Zhou, X. *J. Organomet. Chem.* **2003**, *672*, 94. (d) Zhang, J.; Yi, W.; Chen, Z.; Zhou, X. *Dalton Trans.* **2013**, *42*, 5826. (e) Cao, Y.; Du, Z.; Li, W.; Li, J.; Zhang, Y.; Xu, F.; Shen, Q. *Inorg. Chem.* **2011**, *50*, 3729. (f) Trifonov, A. A.; Fedorova, E. A.; Fukin, G. K.; Bochkarev, M. N.

*Eur. J. Inorg. Chem.* **2004**, 4396. (g) Zhang, W.-X.; Nishiura, M.; Hou, Z. *Synlett* **2006**, 1213. (h) Trifonov, A. A.; Lyubov, D. M.; Fedorova, E. A.; Skvortsov, G. G.; Fukin, G. K.; Kurskii, Yu. A.; Bochkarev, M. N. *Russ. Chem. Bull.* **2006**, *55*, 435. (i) Heitmann, D.; Jones, C.; Junk, P. C.; Lippert, K.-A.; Stasch, A. *Dalton Trans.* **2007**, 187. (j) Ge, S.; Meetsma, A.; Hessen, B. *Organometallics* **2008**, *27*, 3131. (k) Zhang, Z.; Roesky, H. W.; Schulz, T.; Stalke, D.; Doering, A. *Eur. J. Inorg. Chem.* **2009**, 4864. (l) Heitmann, D.; Jones, C.; Mills, D. P.; Stasch, A. *Dalton Trans.* **2010**, *39*, 1877. (m) Basalov, I. V.; Lyubov, D. M.; Fukin, G. K.; Shavyrin, A. S.; Trifonov, A. A. *Angew. Chem., Int. Ed.* **2012**, *51*, 3444. (n) Wang, Y.; Luo, Y.; Chen, J.; Xue, H.; Liang, H. *New J. Chem.* **2012**, *36*, 933.

(16) See the SI for details.

(17) Chen, S.-J.; Dougan, B. A.; Chen, X.-T.; Xue, Z.-L. *Organometallics* **2012**, *31*, 3443.

(18) (a) Bailar, J. C. *J. Inorg. Nucl. Chem* **1958**, *8*, 165. (b) Rahim, M.; Taylor, N. J.; Xin, S.; Collins, S. *Organometallics* **1998**, *17*, 1315. (c) Kakaliou, L.; Scanlon, W. J., IV; Qian, B.; Baek, S. W.; Smith, M. R., III; Motry, D. H. *Inorg. Chem.* **1999**, *38*, 5964. (d) Franceschini, P. L.; Morstein, M.; Berke, H.; Schmalle, H. W. *Inorg. Chem.* **2003**, *42*, 7273.

(19) Sun, J.; Chen, S.; Duan, Y.; Li, Y.; Chen, X.; Xue, Z. *Organometallics* **2009**, *28*, 3088.

(20) (a) Macomber, R. S. *A Complete Introduction to Modern NMR Spectroscopy*; Wiley: New York, 1998; pp 158−160. (b) The rate constants here are the chemical rate constants, and they differ from the observed magnetization transfer rate constants by a factor of 2. See, for example: Green, M. L. H.; Wong, L.-L.; Sella, A. *Organometallics* **1992**, *11*, 2660.

(21) See, for example: (a) Wood, C. D.; McLain, S. J.; Schrock, R. R. *J. Am. Chem. Soc.* **1979**, *101*, 3210. (b) Smith, G. M.; Carpenter, J. D.; Marks, T. J. *J. Am. Chem. Soc.* **1986**, *108*, 6805. (c) McDade, C.; Green, J. C.; Bercaw, J. E. *Organometallics* **1982**, *1*, 1629. (d) Bulls, A. R.; Schaefer, W. P.; Serfas, M.; Bercaw, J. E. *Organometallics* **1987**, *6*, 1219. (e) Rothwell, I. P. *Acc. Chem. Res.* **1988**, *21*, 153. (f) Buchwald, S. L.; Nielson, R. B. *J. Am. Chem. Soc.* **1988**, *110*, 3171. (g) Caulton, K. G.; Chisholm, M. H.; Streib, W. E.; Xue, Z.-L. *J. Am. Chem. Soc.* **1991**, *113*, 6082. (h) Li, L.; Hung, M.; Xue, Z. *J. Am. Chem. Soc.* **1995**, *117*, 12746. (i) Abbott, J. K. C.; Li, L.; Xue, Z.-L. *J. Am. Chem. Soc.* **2009**, *131*, 8246. (j) Sharma, B.; Chen, S.-J.; Abbott, J. K. C.; Chen, X.-T.; Xue, Z.-L. *Inorg. Chem.* **2012**, *51*, 25.

(22) (a) Seetula, J.; Kalliorinne, K.; Koskikallio, J. *J. Photochem. Photobiol., A.: Chem.* **1988**, *43*, 31. (b) Hancock, K. G.; Dickinson, D. A. *J. Org. Chem.* **1975**, *40*, 969. (c) Zhang, X.-H.; Chen, S.-J.; Cai, H.; Im, H.-J.; Chen, T.; Yu, X.; Chen, X.; Lin, Z.; Wu, Y.-D.; Xue, Z.-L. *Organometallics* **2008**, *27*, 1338.

(23) Shi, Q.-Z.; Richmond, T. G.; Trogler, W. C.; Basolo, F. *J. Am. Chem. Soc.* **1984**, *106*, 71.

(24) See, for example: Howard, J. A. In *Free Radicals*; Kochi, J. K., Ed.; John Wiley & Sons: New York, 1973; Vol. *II*, Chapter 12.

(25) Barriga, S. *Synlett* **2001**, 563.

(26) (a) Finke, R. G.; Smith, B. L.; Mayer, B. J.; Molinero, A. A. *Inorg. Chem.* **1983**, *22*, 3677. (b) Mancuso, C.; Halpern, J. *J. Organomet. Chem.* **1992**, *428*, C8. (c) Goodwin, J. M.; Olmstead, M. M.; Patten, T. E. *J. Am. Chem. Soc.* **2004**, *126*, 14352.

(27) More, P. M.; Spencer, M. D.; Wilson, S. R.; Girolami, G. S. *Organometallics* **1994**, *13*, 1646.